The shell fabric of Palaeozoic brachiopods: patterns and trends

Facheng Ye, Claudio Garbelli, Shuzhong Shen and Lucia Angiolini

Abstract

The varied microstructures of brachiopod biominerals represent a robust archive to understand the evolution and adaptations of marine calcifiers in time. Therefore, a detailed study of the shell microstructure of Cambrian to Devonian brachiopods from Iran is here presented. The shell of 38 brachiopod species, representatives of 22 families and nine orders, have been analysed using Scanning Electron Microscope (SEM) and a database has been built, including macro- and micro-morphological features used to characterize the two- or three-layered brachiopod shells. Two main microstructural variants of the secondary layer have been analysed: fibrous and laminar fabrics. The fibrous layer has a fabric comparable to that of recent brachiopods, whereas the laminar fabric is more complex in its structural organization and has no recent analogue. In cross section, the laminae are thinner than the fibres, and much less variable in size. There is evidence that taxa with laminar microstructure have diverged from the Billingsellida and then followed a trend implying a decrease in thickness of the laminae.

Our Linear Discriminant Analysis (LDA) shows that shell fabric and shell thickness are powerful predictors of shell shapes, which in turn approximate the brachiopod lifestyles and ecological strategies. Taxa with a fibrous fabric are mostly biconvex, whereas the groups with a laminar secondary layer are associated to a variety of shell shapes and lifestyles. Even if the relations between shell fabric and shell thickness remain enigmatic, as well as the metabolic cost they imply, shell fabrics, and the possible structural and mechanical

advantages conferred, could have played a role in the evolutionary success of the Strophomenata during the Palaeozoic.

Facheng Ye [facheng@uow.edu.au], Dipartimento di Scienze della Terra "A. Desio", Università degli Studi di Milano, Via Luigi Mangiagalli, 34, Milan, Italy; Facheng Ye [facheng@uow.edu.au], School of Earth, Atmospheric and Life Sciences, University of Wollongong, Northfields Ave, Wollongong, NSW 2522 Australia;

Claudio Garbelli [claudio.garbelli@unife.it]. Dipartimento di Fisica e Scienze della Terra,Università di Ferrara, Via Saragat 1, I-44121 Ferrara, Italy;

Shuzhong Shen [szshen@nju.edu.cn]. School of Earth Sciences and Engineering, Nanjing University, 163 Xianlin Avenue, Nanjing 210023, China; Lucia Angiolini [lucia.angiolini@unimi.it]. Dipartimento di Scienze della Terra "A. Desio", Università degli Studi di Milano, Via Luigi Mangiagalli, 34, Milan, Italy.

The calcite shells of brachiopods are well known to be excellent archives of proxies for studying climate and environmental change and reconstructing the state of the oceans in deep time (e.g. Popp *et al.* 1986; Grossman *et al.* 1991; Azmy *et al.* 1998; Parkinson *et al.* 2005; Angiolini *et al.* 2008, 2009; Brand *et al.* 2013; Cusack & Pérez-Huerta 2012; Garbelli *et al.* 2017, 2019; Brand 2018). However, the fidelity of the brachiopod archive and the interpretation of the archived proxies are dependent on the knowledge of the overall structural organization of the shell at different scales, from its general shape to its microstructure, of the ecological strategies of the group and of its evolution in time. Particularly important in this perspective is the analysis of the brachiopod shell microstructure, which is essential to test the archive preservation (e.g. Brand *et al.* 2011), and

notable to derive information on the chemical composition and the state of an ocean (England *et. al.* 2007; Ye *et al.* 2018a, 2019), but also a useful tool to reconstruct the macro-evolutionary history of the phylum (e.g. Williams 1968, 1970; Williams & Brunton 1993; Dewing 2004). In phylogenetic analyses, shell fabrics have been employed mostly at high taxonomic level (Williams 1956; Baker 1990; Williams & Brunton 1993), but it has been suggested that the overall fabric organization has the potential to provide indications also at low taxonomic ranks (Garbelli 2017).

The fabric of the secondary layer is the most identifiable microstructural feature in a brachiopod shell, and the more variable, as it comprises stratiform, tabular laminar, cross-bladed laminar, foliate, and fibrous fabrics (Williams & Cusack 2007). In the early evolutionary history of brachiopod biomineralization, the most significant transformation was the passage from an organophosphatic shell to an organocarbonate one, which characterizes the most successful classes of the Rhynchonelliformea: the Strophomenata and Rhynchonellata (Williams & Cusack 2007). However, the early evolution of the two main microstructural types that form the secondary layer of the Strophomenata and Rhynchonellata shells – i.e., the laminar and fibrous fabrics - remains to be investigated in details.

The typical laminar fabric of the orders of the Class Strophomenata seems to have independently evolved more than one time. Based on the similar nature of their pseudopunctate fabrics, Williams (1968) proposed that the laminae of the Strophomenida originated from the fibrous fabrics of the Plectambonitoidea. On the other hand, Dewing (2004) considered the impunctate laminae of the primitive Orthotetida to be derived from the laminae of the Billingsellida. Brunton (1972) proposed that the Chonetidina of the Order Productida evolved from the Plectambonitoidea, indirectly suggesting that the laminar fabric of the Productida evolved independently from the Strophomenida. Alternatively, the Strophomenida-Productida lineage should have had a common fibrous-like lath ancestor. The

most recent consensus cladogram of the phylum agrees with this last view since the Strophomenata is considered as monophyletic, with the Billingsellida being the most primitive group originated in the Cambrian (Carlson & Leighton 2001; Popov *et al.* 2007; Carlson 2007, 2016).

Since the shell microstructure has the potential to provide information about poorly understood kinship ties (Williams 1970; Brunton 1972; Williams & Cusack 2007; Garbelli 2017), here we use a quantitative approach to investigate some representative brachiopod orders from Cambrian to Devonian. Specific aims of this study are:

1) to quantify the microstructural features of early stocks, some of which are still poorly known;

2) to compare the microstructural organization of these early brachiopod stocks and discuss their evolutionary ties;

3) to assess if there is a pattern suggesting a relationship between shell fabric, shell thickness, and shell shape and ecological strategies and discuss its implications.

Materials and methods

Shell specimens

A total of 94 specimens collected from different localities in Iran (Fig. 1) were selected for this study. The specimens are representative of 38 species belonging to 9 orders, spanning from Cambrian to Devonian (Table 1, S1). Most of the shells are articulated, with only a few of them being incomplete or fragmented, but all the specimens can be identified at generic level, and the shell orientation is still distinguishable. The material is housed at the Dipartimento di Scienze della Terra "A. Desio", Università di Milano and has been collected during several campaigns of field work in Iran. In particular, specimens labelled MRAN and NiB (Table S1) have been acquired based on the funded research contract "*Paleontology and*

Biozonation of Paleozoic Sediments of Central Iran and Zagros Basins" with the Dipartimento di Fisica e Geologia dell'Università di Perugia and the Pars Geological Reserch Center, Tehran (Angiolini, unpublished reports 2013–2016). Specimens labelled KE have been collected during field work in the Kerman region, Central Iran in October 2016 (for details on the section see Percival *et al.* 2009). A few specimens (labelled LA) belong to older collections, housed at the Dipartimento di Scienze della Terra "A. Desio", Università di Milano.

Data collection

All the specimens were measured with a caliper ruler (length, width and height, Fig. 2), and subsequently prepared following the method suggested by Crippa *et al.* (2016). The fossil shells were sectioned along longitudinal or transverse axes; fragile specimens were embedded in epoxy resin before cutting. Sectioned surfaces were smoothed with silicon carbide powder (SiC), etched with 5% hydrochloric acid (HCl) for 10–15 s, then rinsed under tap water and dried. The surfaces were gold-coated and then inspected using a Cambridge S-360 scanning electron microscope with a lanthanum hexaboride (LaB_6) source and operating at an acceleration voltage of 20 kV. The instrument is located at Dipartimento di Scienze della Terra "A. Desio", Università di Milano.

Measurements of the size of the structural units of the fabric (i.e. laminae and fibres) and the thickness of individual valve shell substance (later referred to as shell thickness) of well preserved specimens were performed on SEM images, using the software Photoshop. As the boundaries of each lamina and fibre are not always very neat, and the contact surfaces of each unit (fibre/lamina) are not straight, to reduce the error, the thickness of each structural unit was measured on a set of 5 laminae/fibres dividing the obtained value by 5 (Fig. 3). The

width of fibres was also measured when their outline was well preserved and symmetrical following the indications of Ye et al. (2018a, p.224-225).

Shell thickness has been measured along a longitudinal section of each specimen at half the length of the shell for all the specimens.

Statistical analyses

We conducted a Dunnett's Modified Tukey-Kramer Pairwise Multiple Comparison (Dunnett 1979) to evaluate the differences of the mean thickness of the structural units between Rhynchonelliformean groups at the main nodes of the phylogenetic tree (Carlson 2016). We applied this test because data are normally distributed, but the sample size and the variance is strongly unequal between the groups used for comparison (see Tables S7, S8).

To recognize if there is a pattern indicating a relationship between the shell microstructure and the ecology of the early stocks, we employed a Linear Discriminant Analysis (LDA). Given a number of independent quantitative variable which describe the data, classified in classes using a categorical variable, this method calculates a within-class scatter matrix and a between-class scatter matrix, with the purpose to maximize the between-class measure while minimizing the within-class measure (Martínez & Kak 2001). The outcome are the Linear Discriminants, each of which is a linear function of the measurements (i.e. the predictor variables) by which different groups are best discriminated (Fisher 1936). We employed shell shapes as categorical classes (biconvex, concavo-convex, plano-convex, flat) as a fairly accurate proxy for different ecological strategies (Harper 1997). As predictor variables, beyond the shell microstructure, we included shell thickness, shell size, and aspect ratio (width/length) since these characters are connected to morpho-functional, ecological and phylogenetic aspects of brachiopods (Leighton 1998; Balthasar *et al.* 2020) and they can be assessed in a consistent way on the studied material. For the shell microstructure, we included

the thickness of its basic structural units, since it is promptly and consistently measurable in most of the analysed specimens. For the size, we calculated the log-transformed shell area, where the shell area is the product of measured width and length (Zhang *et al.* 2015). All the measures were standardized to avoid distortion of the LDA, caused by the different scale of variables. Before preforming the analysis, we inspected the statistical distribution and verify that the data are normally distributed and homoscedastic. We also validated the poor level of correlation between the predictors (Table S6).

To test how well the variables can predict the shape of the shell (i.e. the ecology), we divided the data into two random subsets. The largest comprised 80% of the observations and it was used to build the model. The remaining data were used to quantify how good the model is to predict the shape. All the calculations were performed using R. 3.5.1.

Results

Generally, the primary layer is not preserved in the specimens under investigation (Figs. S1–S10). Two main types of secondary layer fabrics (laminar and fibrous) were observed, plus a unique laminar microstructure in taxa of Chonetidina, all of which are described below.

Laminar fabric

Four investigated orders have a laminar secondary layer. The basic units of the laminae are flat-lying crystallites in the Billingsellida (Figs. 4A, 5B, S1C, S1F), and lath-shaped (blades) crystallites in the Strophomenida, Productida and Triplesiidina (Figs. 6B, 6F, 6G, 6I, S2H, S3D, S5A). These crystallites amalgamate laterally to form laminae, which are grouped into packages, where the axes of blades are general parallel to each other (e.g. Figs. S2D, S3C). In the Strophomenida, Productida, and Triplesiidina, overlapping groups of packages are oriented with the ‘blades’ axis at different angles (e.g. Figs. 6F, S2G). The mean thickness of the laminae ranges from 1.26 to 2.8 μm (Fig. 7, Table S2). Thicker laminae were observed in Billingsellida, where they also show local thickening in terms of radial folds (Fig. 5) and in

Strophomenida, with values generally exceeding 2 μm, while thinner ones, have been observed in the orders Productida and Triplesiidina (Fig. 7). The thickest and thinnest laminae were measured in *Ingria* sp. ind. (> 5 μm, Figs. S5B, S5D) and *Spinulicosta* sp. ind. (< 1 μm, Figs. S9E, S9F) respectively. In the suborder Chonetidina, unlike the other taxa, the structural features of the laminae are not clearly detectable (Fig. 8), and the cross-bladed pattern was not observed.

Obliquely stacked packages of laminae were occasionally found in several groups (e.g. in Billingsellidae gen. et sp. ind., *Martellia shabdjerehensis*, *Ingria* sp. ind.). Instead of being regularly disposed, some packages of laminae are just obliquely stacked at an acute angle forming wedge-like microstructures (e.g. Figs. S1A, S1D, S2A).

Columnar tertiary layers were observed in the innermost part of the shell in *Leptellina* sp. ind. (Fig. S2E), and *Ingria* sp. ind. (Figs. 6A).

Pseudopunctae crossing the laminar layer were observed in *Leptellina* sp., *Productella* cf. *P. belanskii*, *Productella* sp. ind., *Rhytialosia* sp. ind., *Spinulicosta* sp. ind., and *Striatochonetes* sp. ind. (e.g. Figs. 6C-E, 6H, S2F, S3B, S3F, S3H, S4B). The pseudopunctae are formed by several deflected laminae, in which there is often a calcite core, the taleola (lateral view: Fig. 7H). The maximum diameter of the taleola (core of the pseudopuncta) can be up to 10 μm, while the overall diameter of a pseudopuncta can exceed 30 μm.

Spines were observed in *Martellia shabdjerehensis, Productella* cf. *P. belanskii*, *Productella* cf. *P. subaculeata*, and *Productella* sp. ind. (e.g. Figs. S1H, S3A, S3E, S3G). Spines were hollow, but often filled by secondary calcite or micrite. The diameter of the spines in the analysed taxa of Billingsellida (*Martellia shabdjerehensis*, ca. 50 μm) is significantly narrower than in the analysed Productida (*Productella* cf. *P. belanskii* and *Productella* sp. ind. ca. 100 μm).

Fibrous fabric

The taxa of the five examined orders possess a secondary layer with a fibrous fabric. The basic structural units, the fibres (Figs. 9, 10), have a “keel and saddle” (e.g. Figs. 9G, S6G, S10A) or a sub-diamond outline in cross section (e.g. Fig. 9H). The mean width of fibres spans from 8.4 to 23.0 μm in cross-section; the mean thickness, measured in longitudinal section, varies from 2.5 to 6.0 μm (Fig. 7, Table S3). Specimens of the Orthida have the thinnest observed fibres, with mean values ~ 2.7 μm, and result significant thinner than those of other orders, which are generally > 3.3 μm (Table 2, S3). The thickest fibres were observed in *Spinatrypina* cf. *S. chitralensis* shows the thickest measured fibres, ~6.0 μm. In a different species of the same genus, *Spinatrypina* sp. ind., the mean thickness of the fibres is about 3.6 μm (Table S3). The fibres show an evident variation of the size in different position of the same valve (e.g. *Paralenorthis* sp. ind., Fig. S6H and *Hedeinopsis* sp. ind., Fig. 9I), becoming wider and thicker inwardly. In the umbonal region of *Howellites ultima*, the fibres arrangement gives rise to obliquely stacked structure (Fig. S6C).

The columnar tertiary layer, as well as punctae, were not observed in the taxa belonging to the orders Atrypida and Rhynchonellida. However, a persistent columnar tertiary layer is present in species of Orthida, Pentamerida and Spiriferida, such as *Nicolella actoniae*, *Paralenorthis* sp. ind., *Howellites ultima*, *Isorthis (Ovalella) inflata*, *Cyrtospirifer* sp. ind., and *Uchtospirifer* aff. *Uchtospirifer nalivkini* (e.g. Figs. S6E, S7C, S10H). Punctae were only observed in *Howellites ultima* (Fig. S6F).

Statistical analyses and model

The Dunnett's Modified Tukey-Kramer Pairwise Multiple Comparison shows that there are significant differences in the mean thickness of the structural units at the nodes of the phylogenetic tree (Table 2). The Strophomenata have significant thinner units compared to the Rhynchonellata; a similar result is obtained for the Orthida, which has thinner fibres than

the other derived groups with a fibrous fabric. The Billingsellida shows significantly thicker laminae than other derived groups bearing a laminar fabric.

Counting the frequencies of shell shapes based on the type of fabric, the laminar taxa show a higher frequencies of concavo-convex shape, instead the fibrous have and higher number of biconvex shells (Table 3).

The predictor variables results to follow a normal distribution, excluding the shell thickness, which was log transformed to make the data suitable for the analyses. Once the shell thickness was transformed, all variables were homoscedastic and no significant correlation was detected among them (Table S6). Therefore, the model includes the log of the size, to perform the LDA under robust assumptions. The thickness of structural units and the log of the shell thickness are the variables with the highest absolute values for coefficients of the Linear Discriminants (LDs) 1 and 2 respectively (Table 4). These two LDs return a percentage of groups separation equal to 97.82 %, with the LD1 achieving alone the 80.82%. The Linear Discriminants 1 and 2 plotted in Fig. 11 represents only the observation used to build the model. The accuracy of prediction, calculated using the remaining 20% of the data not included in the model, is equal to 0.875 (i.e. the model predict correctly the 87.5 % of the shapes employing the measured variables). An alternative model including only the two variable describing features of the shell wall, returns an accuracy of prediction equal to 1, instead for the size combined with the aspect-ratio, the accuracy drops to 0.625.

Discussions

Laminar fabric

One of the micro-morphological traits characterizing the class Strophomenata is the laminar secondary layer. In this monophyletic group (Carlson 2016), the fabric organization of the Strophomenida-Productida group probably diverged from a common Billingselloid-like

ancestor (Williams 1970), characterized by laminae with radial folds (Williams & Cusack, 2007). In the Billingsellida, the secondary layer is composed of flat crystallites that are ordered and amalgamated laterally into a succession of laminar plates or sheets, as previously observed by Williams (1970) (Figs. 4, 5B-D). In cross-section, the Billingsellida shows laminae with radial folds (e.g. Figs. 5A, 5D), comparable to those of *Billingsella lindströmi* (Linnarsson) and *Billingsella plicatella* (Walcott 1905) illustrated by Williams (1970).

In turn, the Billingsellida laminar fabric may have originated from the fibrous fabric of the Nisusiidae in the Cambrian (Williams 1970), or it may have derived from the Orthidina [All Nodes Occupied Phylogeny analysis by Carlson (2007)]. Our findings suggest that the Billingsellida laminae with radial folds, may represent a distinct, possibly intermediate, type of fabric; they differ from the laminae of the Strophomenida and Productida as they consists of flat-lying individual units which are not composed by lath-shaped (blades) crystallites (Fig. 4); also they are not arranged in groups of packages oriented with the 'blades' axis at different angles (which is characteristic of the Strophomenida and Productida secondary layer, Figs. 6F, S2G) and they are thicker than those of the Strophomenida and Productida taken together (Table 2); neither are they typical fibres as no sub-diamond or "keel and saddle" structural unit has been found in cross section and they are thinner than the fibres.

According to Williams *et al* (2000a) and Dewing (2004), the Strophomenida is considered to have an intermediate fabric between the Billingsellida and Productida. The average thickness of the laminae of the Strophomenida (ca. 2.2–2.6 μm) is closer to that of the Billingsellida (ca. 2.0–2.8 μm), but it is thicker than that of the Productida (ca. 1.2–1.6 μm) (Fig. 7, Table S2). This may indicate that, in taxonomic groups appearing later in the evolution, the size of the structural units tends to be smaller (Fig. 12). Brunton (1972) has already reported a change of the microstructure size, i.e. the tendency of the structural units to become smaller in "geologically younger" taxa of the Chonetidina. This trend is also evident at a higher

taxonomic level – order and class – based on data from the literature. According to Dewing (2004), Ordovician and Early Silurian representatives of Strophomenida have laminae with a thickness of 4 to 10 μm; Permian Productida taxa have much thinner laminae, 0.2 to 0.6 μm (Garbelli *et al.* 2012; Garbelli 2017). Our data underscore the same tendency, i.e. a decrease in the thickness of the laminae. The Billingsellida and Strophomenida, considered as early representatives of laminar fabric brachiopod taxa, show laminae with a thickness ranging 2.0–2.8 μm, with a maximum value of 5.6 μm (Fig. 7, Table S2). Instead, the Productida, which is a late representative of laminar fabric taxa, has thinner and less variable laminae, with average thickness of 1.3–1.7 μm (excluding the Chonetidina) (Fig. 7, Table S2).

The shell microstructure of the Chonetidina has been described either as an intermediate laminar or a lath-like fibrous fabric (Brunton 1972). For example, *Strophochonetes primigenius* (Twenhofel, 1914) (Ordovician) is described as showing transitional fibre-like element; *Dawsonelloides canadensis* (Billings, 1874) (Devonian) bears lath-like fibres, where the units are only 2–4 μm in width; also *Retichonetes vicinus* (Castelnau, 1843) (Devonian) seems to have "fibres" 8–10 μm wide (Brunton 1972). On the other hand, Carboniferous species, like *Rugosochonetes silleesi* Brunton, 1968, show more distinct lath-like units, which are more similar to a true cross-bladed fabric (Brunton 1972). In this study, in two species of Chonetidina, *Striatochonetes* sp. ind. and *Devonochonetes* sp. ind., the shape of the structural units is more similar to a blade than to a fibre (Figs. S4), and the width of the structural unit (ca. 5–10 μm, Fig. 8) is smaller than that of the fibres (ca. 9–25 μm, Table S2, S3). Therefore, also for Devonian species, the fabric of the secondary layer of the Chonetidina must be described as a laminar one. Since the fabric does not bear well-developed pseudopunctae and clear cross-bladed arrangement, the organization of the fabric appears simpler than that of the Productida (Figs. 6, 8).

In the Productida (excluding the Chonetidina), the typical microstructure of the secondary layer is laminar cross-bladed, and pseudopunctae with taleolae and spine internal cavities are frequently observed to cross this layer (Brunton *et al.* 2000) (Fig. 6). According to Alexander (1999b), laminar pseudopunctate Strophomenata should have had an advantage in deflecting fractures and in shell repair.

In the analysed Productida taxa, the laminae are the thinnest recorded and those with the most uniform thickness (Fig. 7, Table S2). If we base our consideration as a whole on the shape of the structural units, the thickness of the laminae and the fabric organization, these features in the Productida may be considered as the most derived stages of the laminar microstructure evolution.

Only one Orthotetida taxon (*Triplesia alata*) was available for this study and, even if not very well preserved, it shows groups of laminae with different orientation (Figs 6I, S5C). Previous works (Garbelli *et al.* 2012; Garbelli 2017) have shown that representatives of this order have a typical cross-bladed laminar fabric in the Permian.

To summarize, two different types of laminar fabric were observed: (1) laminae formed by flat-lying crystallites, locally thickened by radial folds in the Billingsellida; (2) cross-bladed lamination in the Strophomenida, Productida (excluding the Chonetidina) and Orthotetida; laminar fabric, with no evidence of cross-lamination in the Chonetidina. A tendency towards a decrease in the size of the structural units has been observed, but it is difficult to discern a clear trend in the pattern of microstructural organization, except that it probably reaches the highest degree of complexity in the most derived Productida, confirming previous observations (Garbelli 2017).

Fibrous fabric

Due to diagenetic alteration, the typical sub-diamond shape or "keel and saddle" cross-sections of the fibres was rarely observed (Figs. 9G, S6G, S10A). The size of the fibres measured in this analysis (average thickness ranges from 2.5 to 6.0 μm, average width ranges from 8.4 to 23.0 μm, Table S2) is similar to published data on fossil shells [Angiolini (1993; thickness 2–10 μm, width 8–30 μm), Dewing (2004; thickness 4–5 μm; width 10–25 μm) and Garbelli (2017; width 6–27 μm)] and on Recent shells (Ye *et al.* 2018a, b; width 10–15 μm). Additionally, our observation of a change in fibres size inwardly, i.e. with growth (Figs. 9I, S6H), fits well with the findings of the same trends in recent brachiopods (Ye *et al.* 2018a, b). An order-specific variability of the size of the fibres can be detected based on previously published data (cf. Mackinnon & Williams 1974; Angiolini 1993; Williams & Brunton 1993; Dewing 2004; Garbelli *et al.* 2012; Garbelli 2017). The fibres observed in the Orthida - which evolved very early in the Cambrian (Williams & Harper 2000a, b) - are significantly thinner than those of other orders (Table 2, S3), their thickness average values being 2.5–3.3 μm and width being 9.6–16.6 μm, smaller than those recorded in other fibrous fabric taxa (e.g. Pentamerida, Atrypida, Rhynchonellida, Spiriferida) (Tables 2, S3). If we consider the Orthida as the earliest representative of the Rhynchonellata (Williams *et al.* 2000a; Carlson 2007), we can detect a trend toward an increase in the thickness of the fibres in some of the Palaeozoic groups (Table S3, Fig. 12). However, the largest measurement variations were recorded right on fibrous taxa (Table S3, Fig. 5); these large variations might be partly dependent on the angle at which a fibre is cut (see discussion in Ye *et al.* 2018a, and fig. 5), even if we always tried to cut the specimens at a consistent angle and do the measurements on symmetric fibre profiles. These variations, accompanied with the limited number of available specimens, advise caution in supporting the trend towards an increase in thickness of the fibres during the Palaeozoic, which has not been reported before. One of the main

problems in testing this hypothesis is that there is a change of size and shape of the fibres in each single shell along an ontogenetic direction (from outward to inward, from the umbo to the anterior) (Figs. 9I, S6H), as already envisaged in fossil brachiopods (e.g. Mackinnon & Willliams 1974; Garbelli 2017) and in recent ones (Ye *et al.* 2018a, b).

Not only the size and shape of the individual fibres, but also their organization into the overall shell fabric has the potential to give information on the ontogeny and, thus, to understand the phylogenetic history (Garbelli 2017). In this study, the Orthida *Howellites ultima* and *Paralenorthis* sp. ind. show an obliquely overlapping stacked fabric structure in the umbonal part (Figs. S5B-C), not previously found in other species.

In general, the fibrous shell fabrics have a monotonous microstructural organization (Figs. 9-10), with abrupt changes in the orientation of the fibres only in the umbonal part of the shell, the fibres being nearly parallel to the shell external surface in the central and anterior parts. However, changes in the orientation of the fibres also in the middle part of the shells have been reported in recent brachiopods (Schmahl *et al.* 2004, 2012; Griesshaber *et al.* 2008; Gaspard *et al.* 2018; Ye *et al.* 2018a, 2019).

The columnar tertiary layer is not very common in the studied taxa; it could be detected only in seven species (*Nicolella actoniae, Paralenorthis* sp. ind., *Howellites ultima*, *Isorthis (Ovalella) inflata*, *Clorinda* sp. ind., *Cyrtospirifer* sp. ind., *Uchtospirifer* aff. *Uchtospirifer nalivkini*). A thick (more than 800 μm) columnar layer was observed in the umbonal part of *Clorinda* sp. ind., (Fig. S7C); parallel growth lines were also found in cross section, which are comparable with previous observations (Angiolini *et al.* 2012, 2019; Garbelli 2017). An alternation of secondary and tertiary layer was observed only in *Uchtospirifer* aff. *Uchtospirifer nalivkini* (Fig. S10H). However, the preservation is not always good and the transition between the columnar layer and internal shell filling is not always clear.

Relationships between shell shape, shell thickness, and shell fabric

Ecological adaptations and morphological features are strongly related in organisms with shells consisting of two valves, which have several functional constraints (e.g. Leighton 1998, Alexander 1999a). In modern brachiopods, the type of microstructure is strictly related to the performance of functions such as the resistance to mechanical stresses and the capacity of shell repair (Alexander 1999b; Pérez-Huerta *et al.* 2007; Goetz *et al.* 2009; Ye *et at.* 2018a, 2019). Modern biconvex brachiopods (e.g. terebratulids) with a fibrous fabric shell, because of their consistent crystallographic orientation of calcite crystals, may also possess a high capacity of shock absorbance and of preventing propagation of fracture across the shell (Pérez-Huerta & Reed 2018; Pérez-Huerta *et al.* 2007; Schmahl *et al.* 2008).

The shell thickness of Ordovician and Silurian brachiopods has been proven to reflect environmental conditions, but also to be under phylogenetic control (Balthasar *et al.* 2020) and impose functional constraints on the organisms (Leighton 1998). Flow-channel experiments also indicate that there is a strong relationship between the shell shape and hydrodynamic energy (Shiino 2010; Shiino & Suzuki 2011, 2015; Shiino & Angiolini 2014). In summary, the morphology and size of the valves, their shell thickness, and shell fabric affect the functional performance of the shell (Alexander 1989, 1990; Zuschin *et al.* 2003), thus a link between these characters and the ecological strategies is predictable, as suggested for certain brachiopod taxa (Garbelli 2017).

In this study, 90% of the species with a fibrous layer have a biconvex shell, whereas 67 % of the laminar species have a concavo-convex shell (Table 3, Fig. 13). Indeed, most of the Rhynchonellata (fibrous fabric) occupies a biconvex morphospace which maximises shell internal volume to external surface area (McGhee 1999a; Williams & Carlson 2000), whereas the Strophomenata (laminar fabric) is also non biconvex (McGhee 1999b) and has the most variable shapes (e.g. Williams *et al.* 2000b).

Our LDA model (Fig. 11) points out that not only shell fabric (in terms of thickness of its microstructural units), but also shell thickness are powerful predictors of the shell shape class, which in turn approximates the lifestyle of calcite shelled brachiopods, which are very diversified as shown by Harper & Moran (1997). The biconvex shells mainly relate to pedicle-attached or free-lying epifaunal lifestyles, whereas the concavo-convex and plano-convex shells allowed exploitation of the free seminfaunal lifestyle (= pseudoinfaunal of Harper & Moran, 1997) on one side and or of several strategies of shell cementation, or attachment by mantle fibres or clasping spines to the substrate on the other (e.g. Grant 1966; Rudwick 1970).

Therefore, shell thickness and its fabric can be considered determining factors in shaping the evolutionary adaptations of brachiopods. Alongside, it has been advocated that shell thickness and its fabric, coupled with specific ecological strategies, entails a differential cost on the overall energetic budget of these animals (Garbelli *et al.* 2017, Garbelli 2017, Balthasar *et al.* 2020), because the metabolic cost of calcium carbonate deposition is about 5% of that required for the proteinaceous organic fraction (Palmer, 1992). The amount of costly organic component in a shell depends on its fabric, and on the size of the structural units (Garbelli 2015; Garbelli *et al.* 2017; Ye *et al.* 2018a). If the metabolic cost of shell secretion for recent taxa with fibrous fabric is between 3% and 14% (Watson 2009; Balthasar *et al.* 2020), it should have been higher in taxa with laminar fabric (Garbelli *et al*. 2014, 2017). A higher shell organic content, aside from conferring advantages against predation by enhancing shell elastic strength (Zuschin *et al.* 2003), may have provided a greater capability of shell repair; in fact, high frequencies of shell repair have been observed in the Strophomenata (Alexander 1986b, 1999b; Forcino et al. 2017). Alexander (1999b) pointed out that the laminar layer may have had a similar function of nacre in bivalves to stop propagation of fractures and that pseudopunctae may have served as well to deflect fractures.

422 On the contrary, in a survey of shell breakage and repair in recent Rhynchonellata with
423 fibrous fabric from New Zealand, Harper *et al.* (2019) observed that in general, few
424 individuals are able to repair shell damage, and most of the breakages are fatal.
425 Therefore, the organic rich laminar shell fabric may have been one of the key characters in
426 determining the variety of shell shapes and life styles adopted by the Strophomenata and its
427 ability in shell repair and surviving predation; a quick snapshot of this variety is neatly shown
428 in plates 13.1-13.5 of Seilacher & Gishlick (2015, p. 205-213). Even if the brachiopods had
429 already acquired many of their life styles by the Middle Cambrian (Topper *et al.* 2017), the
430 Strophomenata reached an extreme diversification in shell shapes and life styles in the
431 Carboniferous-Permian with the Productida. The most elaborate adaptations were exploited
432 by the Permian coral-like richthofenioids and bizarre lyttoniidines (Wardlaw *et al.* 2000;
433 Williams *et al*. 2000b), both taxa characterized by a laminar fabric. Balthasar *et al.* (2020)
434 have shown that the Strophomenata included both thick- and thin-shelled species and had the
435 largest variety of shell thicknesses, which is consistent with the observations above.
436 Shell fabric was also suggested to be one of the factor responsible of the differential response
437 of brachiopods during the Late Permian global change, which ended up with the selective
438 extinction of the Productida during the end-Permian crisis (Garbelli *et al.* 2017).
439 Even if we did not find any significant correlation between shell thickness and the thickness
440 of the structural units in our dataset (Table S6), a complex interaction between these two
441 features is likely, since a failure to fulfill some of the functional or energy requirements of
442 specific ecological types could be detrimental for the survivorship.
443 Remarkably, brachiopod taxa seem to have employed different solutions to obtain shell
444 thickening. For example, many spiriferids thicken their shell producing a massive columnar
445 layer or by convolution of the secondary layer fibres (Angiolini *et al.* 2008), instead,
446 productids show taxa with shell thickened by thin laminae with a sub-micrometric thickness,

as well as producing thick prismatic layers (Angiolini *et al.* 2012, 2019; Garbelli 2017). In any case, there is never a simple solution such as obtaining a thicker shell by increasing the size of its structural units, as in our data set there is no correlation between shell thickness and fibre/laminae thickness at specific level, nor in most of the orders (Table 5), except for the Orthida which shows a negative correlation at the limit of significance (p=0.05). Interestingly, Garbelli *et al.* (2017, fig. DR6) found a negative correlation between shell thickness and fibres size in a Permian spiriferid species (*Paracrurithyris* sp.) and Balthasar *et al.* (2020) showed that the early stocks, as the Orthida or the Ordovician Strophomenata, have a thicker shell substance than the other groups, implying a more costly shell secretion.

Both the thickness of the structural units and the shell thickness show significant differences at the order level, suggesting that, beyond a functional intrinsic link between thickness and microstructure, phylogenetic constraints affect these features.

The observed differences in shell fabrics, and thus shell shape and ecological strategy, should be related to the underlying biomineralization process. Recently Simonet Roda *et al.* (2019a, b) have provided an extremely detailed multidisciplinary analysis of the formation of the secondary layer fibres in recent brachiopods and offered a model which revise the traditional view of Williams (1966, 1968, 1997). In the model by Simonet Roda *et al.* (2019a, b) , fibre formation results from the activity of several outer epithelial cells, and each fibre, not only is not produced by a single cell, but it is not encased in a single membrane; also Simonet Roda *et al.* (2019b) did not find evidence of an amorphous precursor during fibres secretion.

It is impossible to acquire a comparable knowledge about the biomineralization process of the extinct Strophomenata, but, assuming that it had a similar mechanism of shell formation, their laminar fabrics, characterized by smaller structural units, could arise from a higher degree of organic matrix compartmentalisation, and possibly form via an amorphous precursor. Organic matrices are, in fact, mineralization sites under chemical, spatial,

structural, and morphological control that regulate mineral deposition and ultimately the shape of the exoskeletons (Mann 2001).

Conclusions

Based on very detailed microstructural observations in representative brachiopod taxa from the Cambrian to the Devonian, the following conclusions can be drawn out:

1. A key difference between laminar and fibrous fabrics is related to the size of the structural units; the laminae are significantly thinner than the fibres; the latter are also more variable in their overall size (i.e. they show a larger range of variability), whereas the thickness of the laminae is rather uniform;

2. our research supports that taxa with laminar microstructure diverged from the Billingsellida as hypothesised by Williams & Harper (2000a) and that there is a trend implying a decrease in thickness of the structural units from the primitive taxa to the most derived taxa with laminar fabric;

3. the Chonetidina acquired a true laminar fabric by the Devonian, indicating that the trend of reduction of the size of structural units occurs in also in this clade since their early representatives seem to have had a fabric composed of larger ‘lath like-fibres’;

4. dimensional trends among taxa with fibrous fabric are more difficult to discern, because the size of fibres is high variable also in the same individual; noteworthy, the earliest representative, the Orthida, has fibres significantly thinner than the other fibrous shelled groups;

5. our data show that the most important predictors of the shell shape and of the intrinsically related ecological strategies, are the shell thickness and the shell fabric. Brachiopods with a fibrous secondary layer are mostly biconvex, whereas brachiopods with a laminar secondary

layer display a variety of shell shapes, entailing diverse epifaunal and seminfaunal lifestyles and a different response to shell repair;

6. the relationships between shell thickness and size of the structural units that compose the shell fabric are very complex and have important consequences on the metabolic costs of shell secretion, suggesting the need of further investigation.

Acknowledgements

This project was supported by the European Union's Horizon 2020 research and innovation programme under Marie Skłodowska-Curie grant agreement no. 643084 (BASE–LiNE Earth). We warmly thank Maryamnaz Bahrammanesh of GSI for support during field work in Iran. We acknowledge technical supports by Curzio Malinverno and Agostino Rizzi (Università di Milano) for specimen preparation and SEM analysis. We thank an anonymous reviewer and Uwe Balthasar for their very helpful suggestions on an earlier draft of this paper.

References

Aldridge, A.E. & Gaspard, D. 2011: Brachiopod life histories from spiral deviations in shell shape and microstructural signature – preliminary report. *Memoirs of the Association of Australasian Palaeontologists 41*, 257–268.

Alexander, R.R. 1986a: Life orientation and post-mortem reorientation of Chesterian brachiopod shells by paleocurrents. *Palaios 1*, 303–311.

Alexander, R.R. 1986b: Resistance to and repair of shell breakage induced by durophages in Late Ordovician brachiopods. *Journal of Paleontology 60*, 273–285.

Alexander, R.R. 1989: Influence of valve geometry, ornamentation, and microstructure on fractures in Late Ordovician brachiopods. *Lethaia 22*, 133–147.

521 Alexander, R.R. 1990: Mechanical strength of shells of selected extant articulate
522 brachiopods: Implications for Paleozoic morphologic trends. *Historical Biology 3*, 169–
523 188.
524 Alexander, R.R. 1999a: Function of external skeletal characteristics of articulate brachiopods.
525 In Savazzi, E. (ed.): *Functional morphology of the invertebrate skeleton*, 371–398.
526 Wiley & Sons, Chichester, New York.
527 Alexander, R.R. 1999b: Function of shell microstructure and internal morphology of
528 articulate brachiopods. In Savazzi, E. (ed.): *Functional morphology of the invertebrate*
529 *skeleton*, 399–414. Wiley & Sons, Chichester, New York.
530 Alexander, R.R. 2001: Functional morphology and biomechanics of articulate brachiopod
531 shells. *Paleontological Society Papers 7*, 145–169.
532 Angiolini, L. 1993: Ultrastructure of some Permian and Triassic Spiriferida and Arthyridida
533 (Brachiopoda). *Rivista Italiana di Paleontologia e Stratigrafia 9*, 283–306.
534 Angiolini, L., Darbyshire, D.P.F., Stephenson, M.H., Leng, M.J., Brewer, T.S., Berra, F. &
535 Jadoul. F. 2008: Lower Permian brachiopods from Oman: their potential as climatic
536 proxies. *Earth and Environmental Science Transactions of the Royal Society of*
537 *Edinburgh 98*, 327–344.
538 Angiolini, L., Jadoul, F., Leng, M.J., Stephenson, M.H., Rushton, J., Chenery, S. & Crippa,
539 G. 2009: How cold were the Early Permian glacial tropics? Testing sea-surface
540 temperature using the oxygen isotope composition of rigorously screened brachiopod
541 shells. *Journal of the Geological Society 166*, 933–945.
542 Angiolini, L., Stephenson, M., Leng, M., Jadoul, F., Millward, D., Aldridge, A., Andrews, J.,
543 Chenery, S. & Williams, G. 2012: Heterogeneity, cyclicity and diagenesis in a
544 Mississippian brachiopod shell of palaeoequatorial Britain. *Terra Nova 24*, 16–26.

545 Angiolini, L., Crippa, G., Azmy, K., Capitani, G., Confalonieri, G., Porta, G.D., Griesshaber,
546 E., Harper, D.A.T., Leng, M.J., Nolan, L., Orlandi, M., Posenato, R., Schmahl, W.W.,
547 Banks, V.J. & Stephenson, M.H. 2019: The giants of the phylum Brachiopoda: a matter
548 of diet? *Palaeontology 62*, 889–917.
549 Azmy, K., Veizer, J., Bassett, M.G. & Copper, P. 1998: Oxygen and carbon isotopic
550 composition of Silurian brachiopods: implications for coeval seawater and glaciations.
551 *Geological Society of America Bulletin 110*, 1499–1512.
552 Baker, P.G. 1990: The classification, origin and phylogeny of thecideidine brachiopods.
553 *Palaeontology 33*, 175–191.
554 Baker, P.G. 1991: Morphology and shell microstructure of Cretaceous thecideidine
555 brachiopods and their bearing on thecideidine phylogeny. *Palaeontology 34*, 815–836.
556 Balthasar, U., Jin, J., Hints, L. & Cusack, M. 2020: Brachiopod shell thickness link
557 environment and evolution. *Palaeontology 63,* 171–183.
558 Bassett, M.G., Popov, L.E. & Egerquist, E. 2008: Early ontogeny of some Ordovician–
559 Silurian strophomenate brachiopods: significance for interpreting evolutionary
560 relationships within early Rhynchonelliformea. *Fossils and Strata 54*, 13–20.
561 Brand, U. 2018: Modern and fossil brachiopods: superheroes of archives. 8th International
562 Brachiopod Congress Milan, 11–14 September 2018, *Permophiles 66*, 29.
563 Brand, U., Logan, A., Bitner, M.A., Griesshaber, E., Azmy, K. & Buhl, D. 2011: What is the
564 ideal proxy of Palaeozoic seawater chemistry? *Memoirs of the Association of*
565 *Australasian Palaeontologists 41*, 9–24.
566 Brand, U., Azmy, K., Bitner, M.A., Logan, A., Zuschin, M., Came, R. & Ruggiero, E. 2013:
567 Oxygen isotopes and $MgCO_3$ in brachiopod calcite and a new paleotemperature
568 equation. *Chemical Geology 359*, 23–31.

569 Brunton, H.C. 1972: The shell structure of chonetacean brachiopods and their ancestors.
570 *Bulletin of the British Museum (Natural History) Geology 21*, 1–26.
571 Brunton, C.H.C., Lazarev, S.S. & Grant, R.E. 2000: Productida. In Kaesler, R.L. (ed.):
572 *Treatise on invertebrate paleontology*. *Part H, Brachiopoda, revised, volume 2*, 350–
573 362. Geological Society of America, Boulder, CO, and University of Kansas Lawrence.
574 Carlson, S.J. & Leighton, L.R. 2001: The phylogeny and classification of
575 Rhynchonelliformea. *Paleontological society papers 7*, 27–52.
576 Carlson, S.J. 2016: The Evolution of Brachiopoda. *Annual Review of Earth and Planetary*
577 *Sciences 44*, 409–438.
578 Carlson, S.J. 2007: Recent research on brachiopod evolution. In Selden, P.A. (ed.): *Treatise*
579 *on Invertebrate Paleontology. Part H, Brachiopoda, revised, volume 6*, 2878–2900.
580 Geological Society of America, Boulder, CO, and University of Kansas Lawrence.
581 Crippa, G., Ye, F., Malinverno, C. & Rizzi, A. 2016: Which is the best method to prepare
582 invertebrate shells for SEM analysis? Testing different techniques on recent and fossil
583 brachiopods. *Bollettino della Società Paleontologica Italiana 55*, 111–125.
584 Curry, G.B. & Brunton, C.H.C. 2007: Stratigraphic distribution of Brachiopods. In Selden,
585 P.A. (ed.): *Treatise on invertebrate paleontology. Part H, Brachiopoda, revised, volume*
586 *6*, 2901–3081. Geological Society of America, Boulder, CO, and University of Kansas
587 Lawrence.
588 Cusack, M. & Pérez-Huerta, A. 2012: Brachiopods recording seawater temperature—A
589 matter of class or maturation? *Chemical Geology 334*, 139–143.
590 Dewing, K. 2004: Shell structure and its bearing on the phylogeny of late Ordovician-early
591 Silurian Strophomenoid brachiopods from Anticosti Island, Québec. *Journal of*
592 *Paleontology 78*, 275–286.

593 Dunnett, C.W. 1979: Pairwise Multiple Comparisons in the Unequal Variance Case. *Journal*
594 *of the American Statistical Association* 75, 796–800.
595 England, J. Cusack, M. & Lee, M.R. 2007: Magnesium and sulphur in the calcite shells of
596 two brachiopods, *Terebratulina retusa* and *Novocrania anomala*. *Lethaia 40,* 2–10.
597 Fisher, R.A. 1936: The use of multiple measurements in taxonomic problems. *Annals of*
598 *Eugenics 7,* 179–188.
599 Fleury, C., Marin, F., Marie, B., Luquet, G., Thomas, J., Josse, C., Serpentini, A. & Lebel,
600 J.M. 2008: Shell repair process in the green ormer *Haliotis tuberculata*: A histological
601 and microstructural study. *Tissue and Cell 40*, 207–218.
602 Forcino, F.L., Stafford, E.S. & Tetreault, R.L. 2017: Brachiopod morphology, life mode, and
603 crushing predation in the Ordovician Arnheim Formation, Kentucky, USA. *Historical*
604 *Biology 31,* 914–925.
605 Garbelli, C., Angiolini, L., Brand, U. & Jadoul, F. 2014: Brachiopod fabric, classes and
606 biogeochemistry: Implications for the reconstruction and interpretation of seawater
607 carbonisotope curves and records: *Chemical Geology 371*, 60–67.
608 Garbelli, C. 2015: Biomineralization and global changes: brachiopod shells as archives of the
609 end Permian events. Milan: Università degli Studi di Milano. PhD thesis
610 Garbelli, C. 2017: Shell microstructures in Lopingian brachiopods: implications for fabric
611 evolution and calcification. *Rivista Italiana di Paleontologia e Stratigrafia 123*, 541–560.
612 Garbelli, C., Angiolini, L., Jadoul, F. & Brand, U. 2012: Micromorphology and differential
613 preservation of Upper Permian brachiopod low–Mg calcite. *Chemical Geology 298*, 1–
614 10.
615 Garbelli, C., Angiolini, L., Brand, U. & Jadoul, F. 2014: Brachiopod fabric, classes and
616 biogeochemistry: Implications for the reconstruction and interpretation of seawater
617 carbon-isotope curves and records. *Chemical Geology 371*, 60–67.

618 Garbelli, C., Angiolini, L. & Shen, S.Z. 2017: Biomineralization and global change: A new
619 perspective for understanding the end-Permian extinction. *Geology 45*, 19–22.
620 Garbelli, C., Shen, S.Z., Immenhauser, A., Brand, U., Buhl, D., Wang, W.Q., Zhang, H. &
621 Shi, G.R. 2019: Timing of Early and Middle Permian deglaciation of the southern
622 hemisphere: Brachiopod-based $^{87}Sr/^{86}Sr$ calibration. *Earth Planetary Science Letters*
623 *516*, 122–135.
624 Gaspard, D., Aldridge, A.E., Boudouma, O., Fialin, M., Rividi, N. & Lécuyer, C. 2018:
625 Analysis of growth and form in *Aerothyris kerguelenensis* (rhynchonelliform
626 brachiopod) - Shell spiral deviations, microstructure, trace element contents and stable
627 isotope ratios. *Chemical Geology 483*, 474–490.
628 Ghaderi, A., Garbelli, C., Angiolini, L., Ashouri, A.R., Korn, D., Rettori, R. & Gharaie,
629 M.H.M. 2014: Faunal change near the end-Permian extinction: the brachiopods of the
630 Ali Bashi Mountains, NW Iran. *Rivista Italiana di Paleontologia e Stratigrafia 120*, 27–
631 59.
632 Goetz, A.J., Griesshaber, E., Neuser, R.D., Lüter, C., Hühner, M., Harper, E. & Schmahl,
633 W.W. 2009: Calcite morphology, texture and hardness in the distinct layers of
634 rhynchonelliform brachiopod shells. *European Journal of Mineralogy 21*, 303–315.
635 Grant, R.E. 1966: Spine arrangement and life habits of the productoid brachiopod
636 Waagenoconcha. *Journal of Paleontology 40*, 1063–1069.
637 Griesshaber, E., Neuser, R.D., Brand, U., Schmahl, W.W. 2008: Texture and microstructure
638 of modern rhynchonellide brachiopod shells – an ontogenetic study. In Rollett, A.D.
639 (ed.): *Application of Texture Analysis: Ceramic Transactions, volume 201*, 605–619.
640 John Wiley and Sons, Inc., Hoboken, New Jersey.

641 Grossman, E.L., Zhang, C. & Yancey, T.E. 1991: Stable–isotope stratigraphy of brachiopods
642 from Pennsylvanian shales in Texas. *Geological Society of America Bulletin 103*, 953–
643 965.
644 Harper, D.A.T. & Moran, R. 1997: Fossils explained 20: Brachiopod life styles. *Geology*
645 *Today 13*, 235–238.
646 Harper, E.M., Lamare, M.D. & Lee, D.E. 2019: Patterns of unrepaired shell damage in recent
647 brachiopods from fiordland (New Zealand). *Rivista Italiana di Paleontologia e*
648 *Stratigrafia 125*, 669–677.
649 Ishikawa, M. & Kase, T. 2007: Multiple predatory drill holes in Cardiolucina (Bivalvia:
650 Lucinidae): Effect of conchiolin sheets in predation. *Palaeogeography,*
651 *Palaeoclimatology, Palaeoecology 254*, 508–522.
652 Joachimski, M.M., Breisig, S, Buggisch, W, Talent, J.A., Mawson, R., Gereke, M., Morrow,
653 J.M., Day, J. & Weddige, K. 2009: Devonian climate and reef evolution: Insights from
654 oxygen isotopes in apatite. *Earth and Planetary Science Letters 284*, 599–609.
655 Kent, D.V. & Keppie, J.D. 1988: Silurian–Permian paleocontinental reconstructions and
656 circum-Atlantic tectonics. In Harris, A.L. & Fettes, D.J. (eds.): *The Caledonian-*
657 *Appalachian orogeny*, 469–480. Geological Society, London, Special Publication No.
658 38.
659 Leighton, L.R. 1998: Constraining functional hypotheses: Controls on the morphology of the
660 concavo-convex brachiopod *Rafinesquina*. *Lethaia 31*, 293–307.
661 Leighton, L.R. 2003: Predation on Brachiopods. In Kelley, P.H., Kowalewski, M. & Hansen,
662 T.A. (eds.): *Predator—Prey Interactions in the Fossil Record, volume 20*, 215–237.
663 Springer, Boston, MA.

664 Livermore, R.A., Smith, A.G. & Briden, J.C. 1985: Palaeomagnetic constraints on the
665 distribution of continents in the Late Silurian and Early Devonian. *Philosophical*
666 *Transactions of the Royal Society of London, B309*, 29–56.
667 Mackinnon, D.I. & Williams, A. 1974: Shell structure of Terebratulid brachiopods.
668 *Palaeontology 17*, 179–202.
669 Mann, S. 2001: *Biomineralization: Principles and Concepts in Bioinorganic Materials*
670 *Chemistry*, 198 pp. Oxford University Press, New York.
671 Martínez, A.M. & Kak, A.C. 2001: PCA versus LDA. *Transactions on Pattern Analysis and*
672 *Machine Intelligence* 23, 228–233.
673 McGhee, G.R.Jr. 1999a: The optimum biconvex brachiopod in the theoretical spectrum of
674 shell form. In Savazzi, E. (ed.): *Functional morphology of the invertebrate skeleton*,
675 415–420. Wiley & Sons, Chichester, New York.
676 McGhee, G.R.Jr. 1999b: The theoretical enigma of non-biconvex brachiopod shell form. In
677 Savazzi, E. (ed.): *Functional morphology of the invertebrate skeleton*, 429–433. Wiley
678 & Sons, Chichester, New York.
679 Parkinson, D., Curry, G.B., Cusack, M. & Fallick, A.E. 2005: Shell structure, patterns and
680 trends of oxygen and carbon stable isotopes in modern brachiopod shells. *Chemical*
681 *Geology 219*, 193–235.
682 Percival, I.G., Wright, A.J., Nicoll, R.S. & Hamedi, M.A. 2009: Martellia and associated
683 Middle Ordovician brachiopods from the Katkoyeh Formation, east-central Iran.
684 *Memoirs of the Association of Australasian Palaeontologists 37*, 315–325.
685 Pérez-Huerta, A., Cusack, M., Zhu, W., England, J. & Hughes, J. 2007: Material properties of
686 brachiopod shell ultrastructure by nanoindentation. *Journal of The Royal Society*
687 *Interface 4*, 33–39.

688 Pérez-Huerta, A. & Reed, H. 2018: Preliminary assessment of coupling the analysis of shell
689 microstructures and microtextures as palaeoecological indicator in fossil brachiopods.
690 *Spanish journal of palaeontology 33*, 129–138.
691 Popov, L.E., Egerquist, E. & Holmer, L.E. 2007: Earliest ontogeny of Middle Ordovician
692 rhynchonelliform brachiopods (Clitambonitoidea and Polytoechioidea): implications for
693 brachiopod phylogeny. *Lethaia 40*, 85–96.
694 Popp, B.N., Anderson, T.F. & Sandberg, P.A. 1986: Brachiopods as indicators of original
695 isotopic compositions in some Paleozoic limestones. *Geological Society of America*
696 *Bulletin 97*, 1262–1269.
697 Rudwick, M.J.S. 1970: *Living and Fossil Brachiopods*, 199 pp. Hutchinson University
698 Library, London.
699 Santosh, M., Maruyama, S. & Yamamoto, S. 2009: The making and breaking of
700 supercontinents: some speculations based on superplume, superdownwelling and the
701 role of tectosphere. *Gondwana Research 15*, 324–341.
702 Schmahl, W.W., Griesshaber, E., Neuser, R., Lenze, A., Job, R. & Brand, U. 2004: The
703 microstructure of the fibrous layer of terebratulide brachiopod shell calcite. *European*
704 *Journal of Mineralogy 16*, 693–697.
705 Schmahl, W.W., Griesshaber, E., Merkel, C., Kelm, K., Deuschle, J., Neuser, R.D., Göetz,
706 A.J., Sehrbrock, A. & Mader, W. 2008: Hierarchical fibre composite structure and
707 micromechanical properties of phosphatic and calcitic brachiopod shell biomaterials–an
708 overview. *Mineralogical Magazine 72*, 541–562.
709 Schmahl, W.W., Griesshaber, E., Kelm, K., Goetz, A., Jordan, G., Ball, A., Xu, D., Merkel,
710 C. & Brand, W. 2012: Hierarchical structure of marine shell biomaterials: biomechanical
711 functionalization of calcite by brachiopods. *Zeitschrift für Kristallographie - Crystalline*
712 *Materials 227*, 793–804.

713 Seilacher A. & Gishlick A.D. 2015: *Morphodynamics*, 551 pp. CRC Press, Taylor & Francis
714 Group, Boca Raton.
715 Shiino, Y. 2010: Passive feeding in spiriferide brachiopods: an experimental approach using
716 models of Devonian *Paraspirifer* and *Cyrtospirifer*. *Lethaia 43*, 223–231.
717 Shiino, Y. & Suzuki, Y. 2011: The ideal hydrodynamic form of the concavo-convex
718 productide brachiopod shell. *Lethaia 44*, 329–343.
719 Shiino, Y. & Suzuki, Y. 2015: A rectifying effect by internal structures for passive feeding
720 flows in a concavo-convex productide brachiopod. *Paleontological Research 19*, 283–
721 287.
722 Shiino, Y. & Angiolini, L. 2014: Hydrodynamic advantages in the free-living spiriferinide
723 brachiopod *Pachycyrtella omanensis*: functional insight into adaptation to high-energy
724 flow environments. *Lethaia 47*, 216–228.
725 Simonet Roda, M., Griesshaber, E., Ziegler, A., Rupp, U., Yin, X., Henkel, D., Häussermann,
726 V., Laudien, J., Brand, U., Eisenhauer, A., Checa, A.G. & Schmahl, W.W. 2019a:
727 Calcite fibre formation in modern brachiopod shells. *Scientific Reports 9*, 598.
728 Simonet Roda, M., E., Ziegler, Griesshaber, E., Yin, X., Rupp, U., Greiner, M., Henkel, D.,
729 Häussermann, V., Eisenhauer, A., Laudien, J. & Schmahl, W.W. 2019b: Terebratulide
730 brachiopod shell biomineralization by mantle epithelial cells. *Journal of Structural*
731 *Biology 207*, 136–157.
732 Topper, T.P., Zhang, Z., Gutiérrez-Marco, J.C. & Harper, D.A.T. 2017: The dawn of a
733 dynasty: life strategies of Cambrian and Ordovician brachiopods. *Lethaia*, https://doi.
734 org/10.1111/let.12229.
735 Wardlaw, B., Grant, R.E. & Brunton, C.H.C. 2000: Richthofenioidea. In Kaesler, R.L. (ed.):
736 *Treatise on Invertebrate Paleontology. Part H, Brachiopoda, revised, volume 3*, 610–
737 619. Geological Society of America, Boulder, CO, and University of Kansas Lawrence.

738 Watson, S.A. 2009: Latitudinal gradients in marine invertebrate shell morphology:
739 production costs and predation pressure. Southampton: University of Southampton,
740 Faculty of Science, School of Ocean and Earth. PhD thesis
741 Williams, A. 1956: The calcareous shell of the Brachiopoda and its importance to their
742 classification. *Biological Reviews 31*, 243–287.
743 Williams, A. 1966: Growth and structure of the shell of living articulate brachiopod. *Nature*
744 *211*, 1146–1148.
745 Williams, A. 1968: Evolution of the shell structure of articulate brachiopods. *Special Papers*
746 *in Palaeontology 2*, 1–55.
747 Williams, A. 1970: Origin of laminar-shelled articulate brachiopods. *Lethaia 3*, 329–342.
748 Williams, A. 1997: Shell structure. In R. L. Kaesler, (ed.): *Treatise on Invertebrate*
749 *Paleontology. Part H, Brachiopoda, revised, volume 1*, 267–320. Geological Society of
750 America, Boulder, CO, and University of Kansas Lawrence.
751 Williams A. & Brunton, C.H.C. 1993: Role of shell structure in the classification of the
752 orthotetidine brachiopods. *Palaeontology 36*, 931–966.
753 Williams A. & Carlson, S.J. 2000: Rhynchonellata. In Kaesler, R.L. (ed.): *Treatise on*
754 *Invertebrate Paleontology. Part H, Brachiopoda, revised, volume 3*, 708–846.
755 Geological Society of America, Boulder, CO, and University of Kansas Lawrence.
756 Williams, A. & Harper, D.A.T. 2000a: Billingsellida. In Kaesler, R.L. (ed.): *Treatise on*
757 *Invertebrate Paleontology. Part H, Brachiopoda, revised, volume 3*, 689–708.
758 Geological Society of America, Boulder, CO, and University of Kansas Lawrence.
759 Williams, A. & Harper, D.A.T. 2000b: Orthida. In Kaesler, R.L. (ed.): *Treatise on*
760 *Invertebrate Paleontology. Part H, Brachiopoda, revised, volume 3*, 714–723.
761 Geological Society of America, Boulder, CO, and University of Kansas Lawrence.

762 Williams, A., Carlson, S.J. & Brunton, C.H.C. 2000a: Brachiopod classification. In Kaesler,
763 R.L. (ed.): *Treatise on Invertebrate Paleontology. Part H, Brachiopoda, revised, volume*
764 *2*, 1–27. Geological Society of America, Boulder, CO, and University of Kansas
765 Lawrence.
766 Williams, A., Howard, C., Brunton, C.H.C. & Cocks, L.R.M. 2000b: Strophomenata. In
767 Kaesler, R.L. (ed.): *Treatise on Invertebrate Paleontology. Part H, Brachiopoda,*
768 *revised, volume 2*, 215–708. Geological Society of America, Boulder, CO, and
769 University of Kansas Lawrence.
770 Williams, A. & Cusack, M. 2007: Chemicostructural diversity of the brachiopod shell. In
771 Selden, P.A. (ed.): *Treatise on Invertebrate Paleontology, Part H, Brachiopoda, revised,*
772 *volume 6*, 2396–2521. Geological Society of America, Boulder, CO, and University of
773 Kansas Lawrence.
774 Ye, F., Crippa, G., Angiolini, L., Brand, U., Capitani, G., Cusack, M., Garbelli, C.,
775 Griesshaber, E., Harper, E. & Schmahl, W. 2018a: Mapping of recent brachiopod
776 microstructure: a tool for environmental studies. *Journal of Structural Biology 201*,
777 221–236.
778 Ye, F., Crippa, G., Garbelli, C. & Griesshaber, E. 2018b: Microstructural data of six recent
779 brachiopod species: SEM, EBSD, morphometric and statistical analyses. *Data in Brief*
780 *18*, 300–318.
781 Ye, F., Jurikova, H., Angiolini, L., Brand, U., Crippa, G., Henkel, D., Laudien, J., Hiebenthal,
782 C. & Šmajgl, D. 2019: Variation in brachiopod microstructure and isotope geochemistry
783 under low pH–ocean acidification–conditions. *Biogeosciences 16*, 617–642.
784 Zhang, Z., Augustin, M. & Payne, J.L. 2015: Phanerozoic trends in brachiopod body size
785 from synoptic data. *Paleobiology 41*, 491–501.

786 Zuschin, M., Stachowitsch, M. & Stanton Jr, R.J. 2003: Patterns and processes of shell
787 fragmentation in modern and ancient marine environments. *Earth-Science Reviews 63*,
788 33–82.

789

Fig. 1. Sampling localities of fossil brachiopods in Iran.

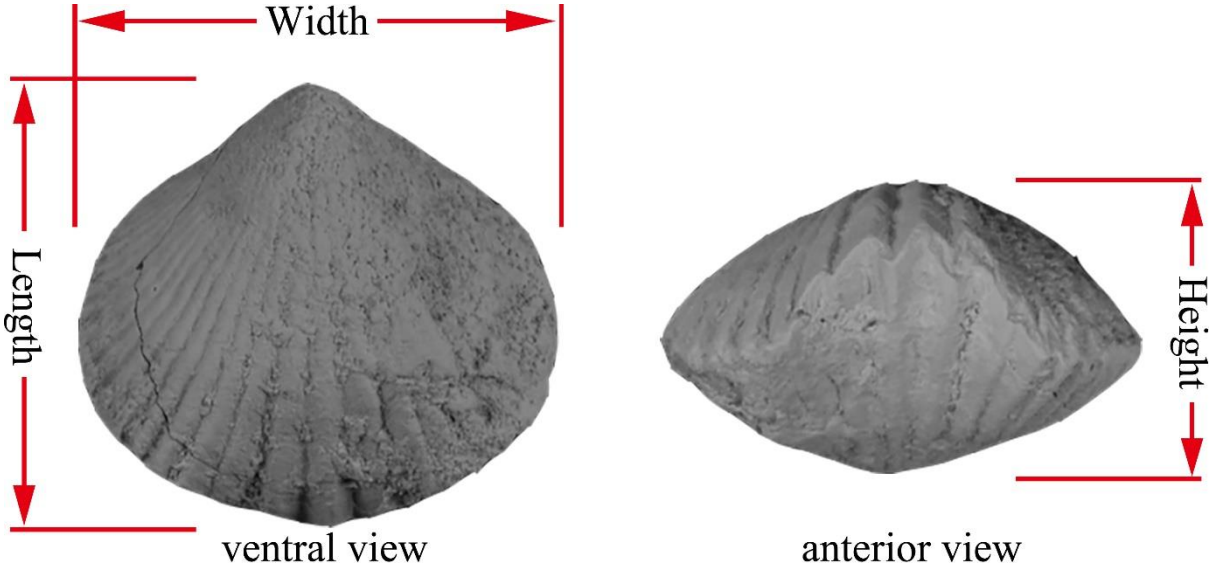

Fig. 2. Acquired measurements to estimate the size of brachiopod shell.

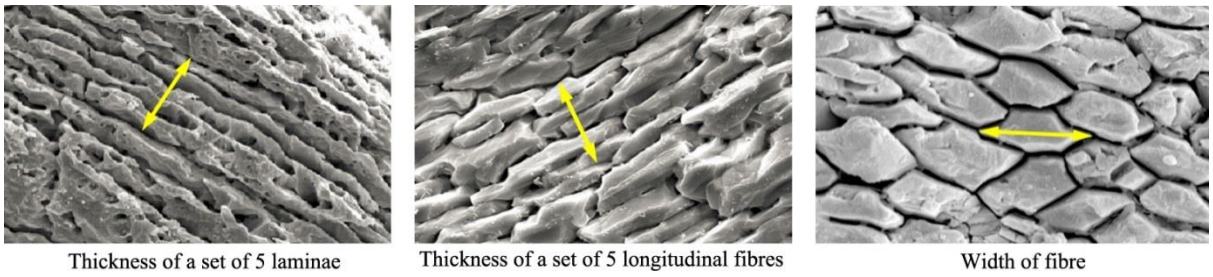

Fig. 3. Measurements to estimate the size of the laminae and fibres.

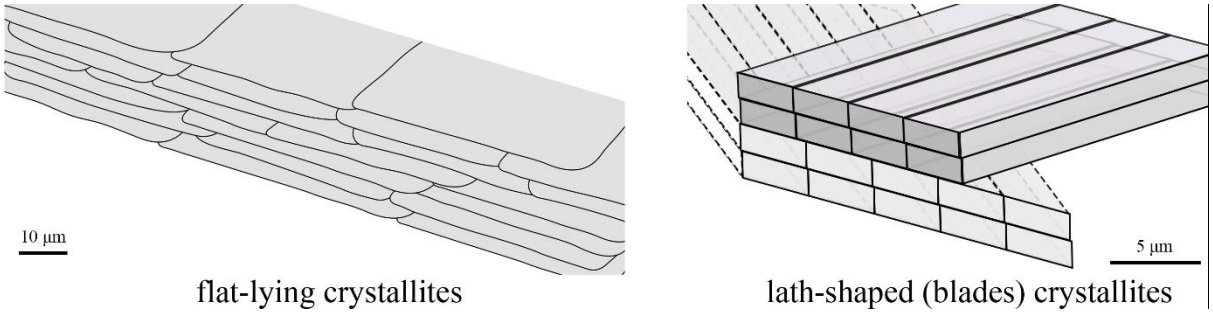

Fig. 4. Schematic illustration showing organization of laminar fabric: 'flat-lying crystallites' (typical of Billingsellida, reconstructed based on Fig. S1C) and 'lath-shaped (blades) crystallites' (typical of Strophomenida and Productida, reconstructed based on Figs. 6F, S2G). Note that the two sketches are drawn at different scales.

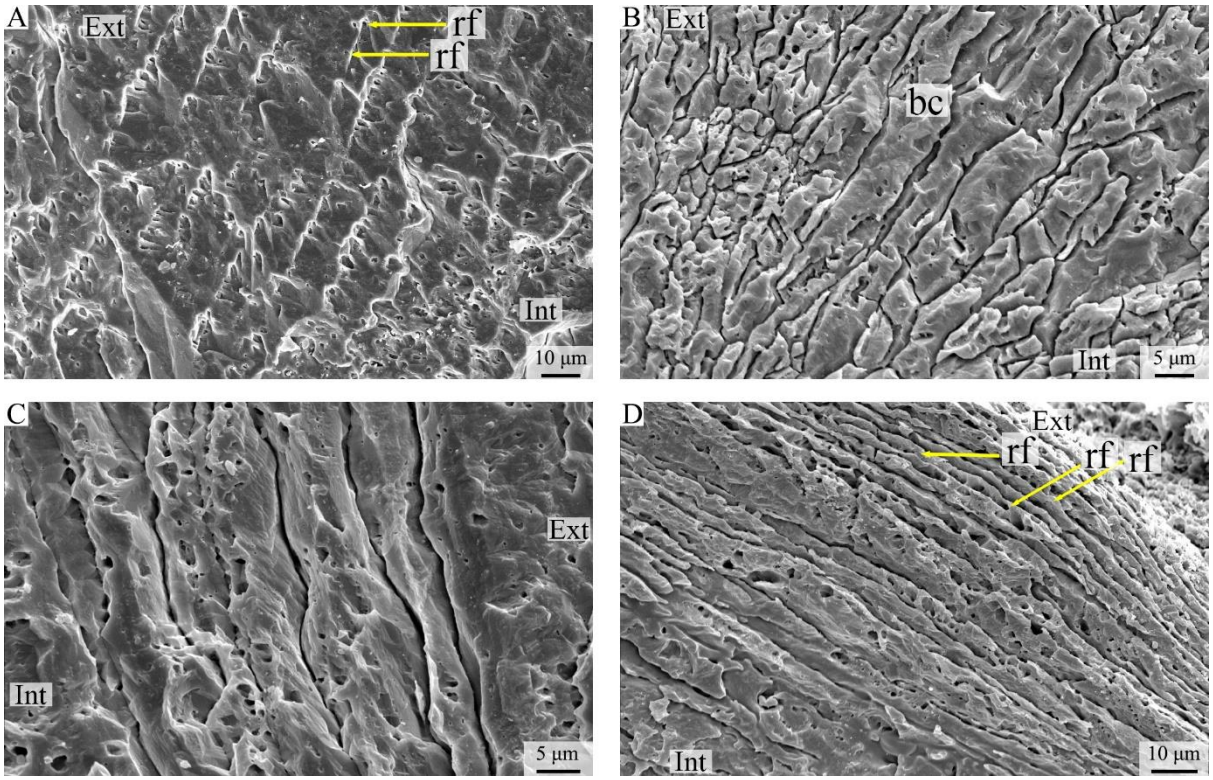

Fig. 5. A: Laminae seen from above, near the posterior part of the shell (*Billingsella* aff. *B. seletensis*, MRAN 898-3-3, ventral valve); B: detail of the laminae (Billingsellidae gen. et sp. ind., MRAN 8760-2, ventral valve); C: enlarged detail of laminae (Billingsellidae gen. indet., MRAN 8760-1, dorsal valve); D: laminar layer near the posterior part of the shell (*Protambonites* cf. *P. primigenius*, MRAN 8763-2, ventral valve). Ext: external part of the shell; Int: internal part of the shell; rf: radial fold; bc: blocky calcite.

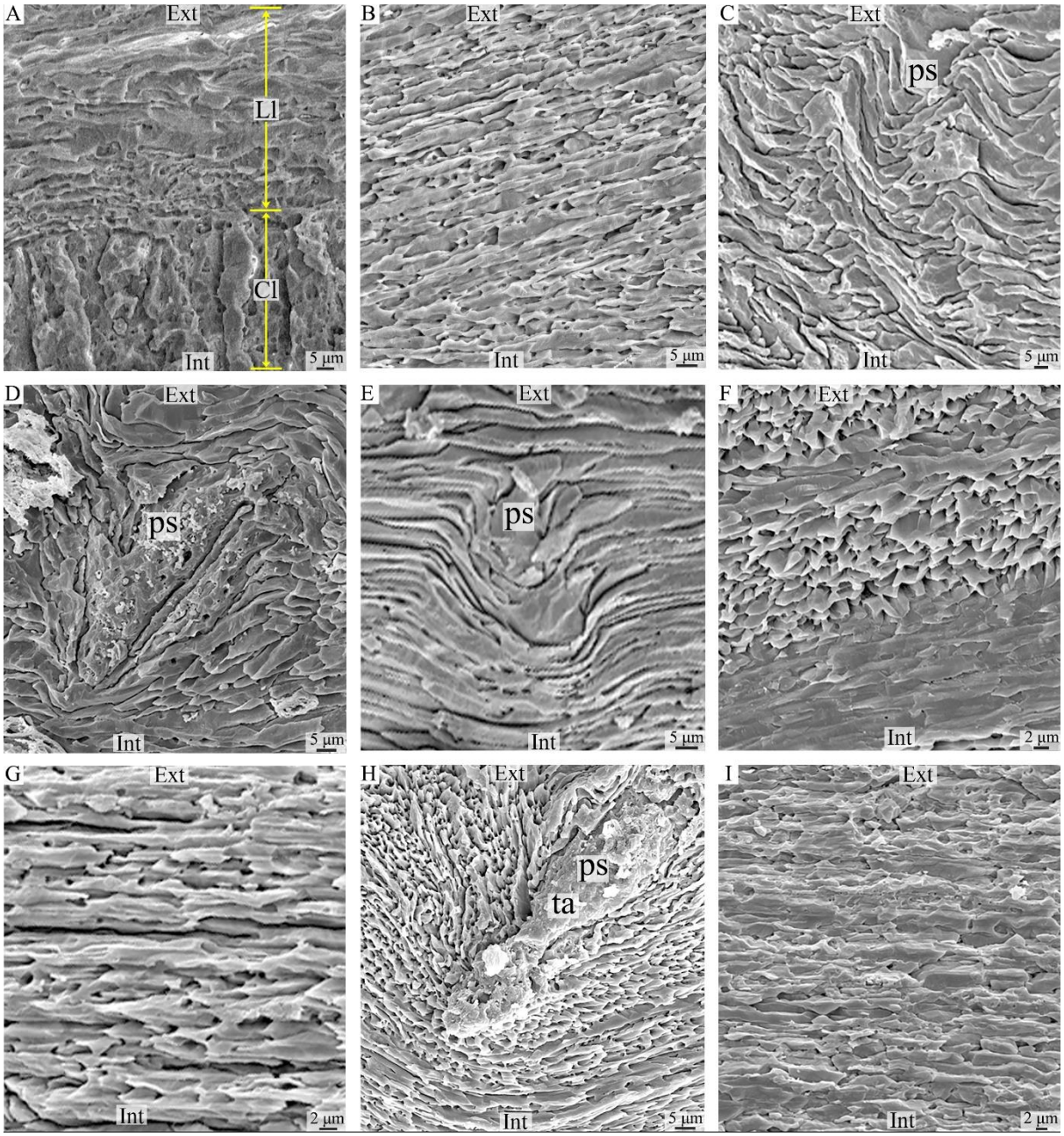

Fig. 6. A: transition between laminar secondary layer and columnar tertiary layer (*Ingria* sp. ind., MRAN 1108-2C, ventral valve); B: laminar layer near the anterior part of the shell (*Ingria* sp. ind., MRAN 1108-2C, ventral valve); C-E: pseudopunctae in posterior, central, anterior part of the shell respectively (*Leptellina* sp., KE-45-4, ventral valve); F, G: cross-bladed laminar layer (*Spinulicosta* sp. ind. MRAN 6162-21, ventral valve); H: pseudopuncta (*Spinulicosta* sp. ind., MRAN 6162-21, dorsal valve); I: laminar layer (*Triplesia alata,* MRAN 1181-7, ventral valve). Ll: Laminar layer; Cl: Columnar layer; ps: pseudopuncta; ta: taleola; Ext: external part of the shell; Int: internal part of the shell.

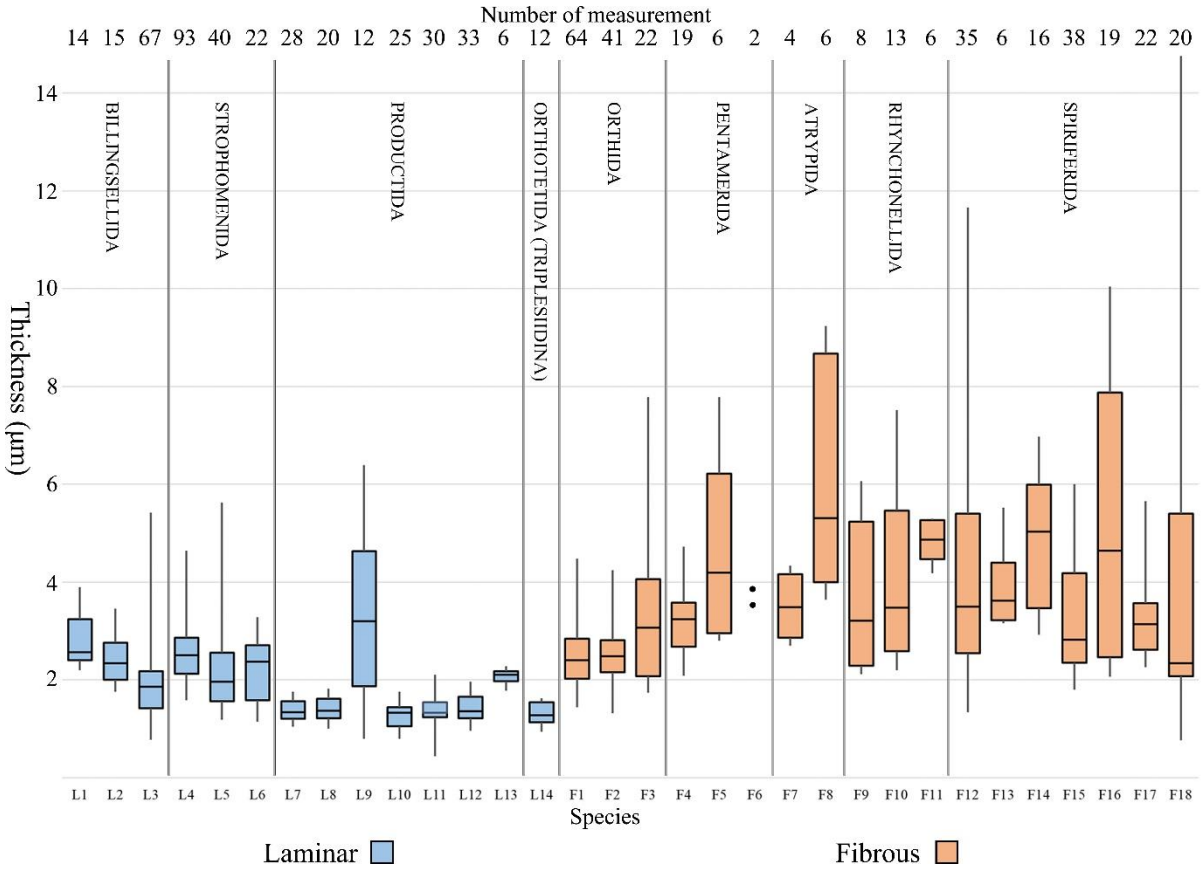

Fig. 7. Comparison of the thickness of laminae and fibres respectively in the laminar and fibrous fabric taxa, each bar represents one species, L1: Billingsellidae gen. et sp. ind., L2: *Protambonites* cf. *P. primigenius,* L3: *Martellia shabdjerehensis,* L4: *Leptellina* sp. ind., L5: *Ingria* sp. ind., L6: *Leptaena depressa,* L7: *Productella* cf. *P. belanskii,* L8: *Productella* cf. *Productella subaculeata,* L9: *Productella* sp. ind., L10: *Rhytialosia* sp. ind., L11: *Spinulicosta* sp. ind., L12: *Striatochonetes* sp. ind., L13: *Devonochonetes* sp. ind., L14: *Triplesia alata,* F1: *Nicolella actoniae,* F2: *Paralenorthis* sp. ind., F3: *Howellites ultima,* F4: *Isorthis (Ovalella) inflate,* F5: *Isorthis* sp. ind., F6: *Clorinda* sp. ind., F7: *Clorinda molongensis,* F8: *Spinatrypina* cf. *S. chitralensis,* F9: *Spinatrypina* sp. ind., F10: *Rhynchotrema* sp. ind., F11: *Stegocornu denisae,* F12: *Cyphoterorhynchus arpaensis,* F13: *Hedeinopsis hispanica hispanica,* F14: *Hedeinopsis* sp. ind., F15: *Cyrtospirifer brodi,* F16: *Cyrtospirifer* cf. *C. kermanensis,* F17: *Cyrtospirifer* sp. ind., F18: *Uchtospirifer* aff. *Uchtospirifer nalivkini.* The bottom/top lines of the box are the first/third quartiles of the data of each individual species, while the band line inside is the median value; ends of the whiskers represent the maximum and minimum of data.

*F6: *Clorinda* sp. ind. only has two measurement data, plotted as individual data points here.

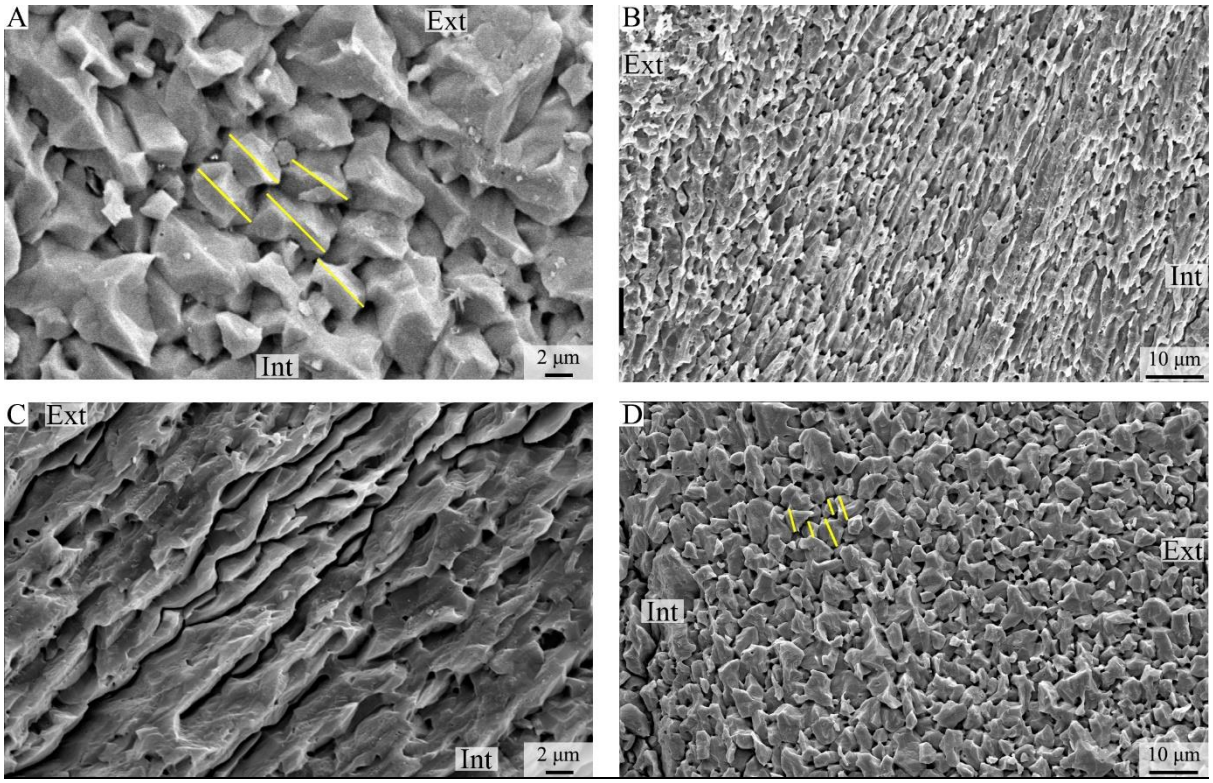

Fig. 8. A: detail of laminae (*Devonochonetes* sp. ind., MRAN 3648-13, ventral valve); B: laminar layer in the central part of the shell (*Striatochonetes* sp. ind., MRAN 9136-3, ventral valve); C: detail of the laminae (*Striatochonetes* sp. ind., MRAN 9159-2, ventral valve); D: laminar layer (*Devonochonetes* sp. ind., MRAN 3648-4, ventral valve); Ext: external part of the shell; Int: internal part of the shell. Yellow line: measured unit width.

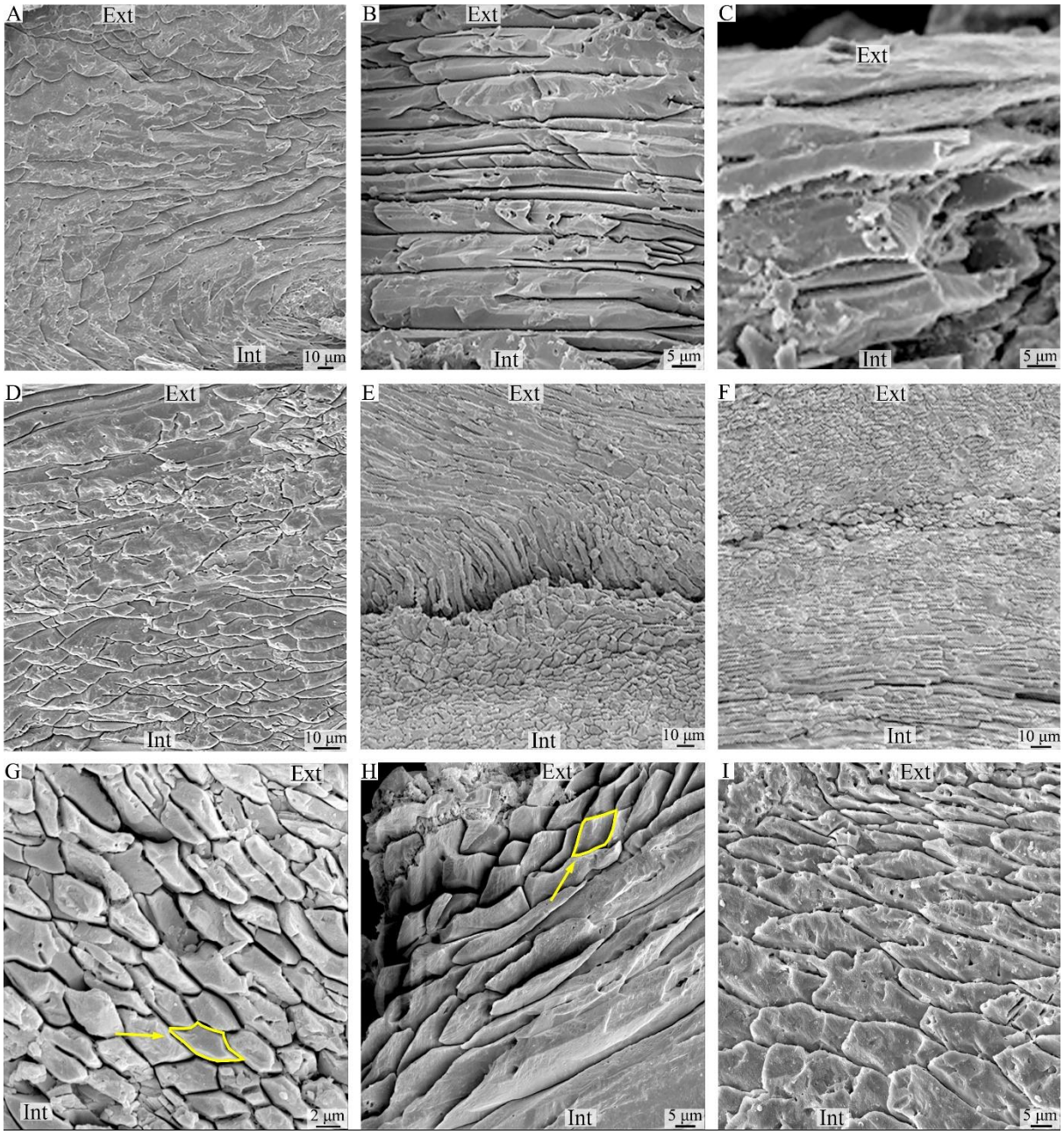

Fig. 9. A, B: fibrous layer in the posterior and central part of the shell respectively (*Spinatrypina* sp. ind. MRAN 1180-3, ventral valve); C: fibrous layer in the external part of the shell (*Spinatrypina* sp. ind. NiB5-2-S, ventral valve); D: fibrous layer in the posterior part of the shell (*Cyrtospirifer brodi*, MRAN 6162-12, *ventral valve*); E, F: fibrous layer in the central part of the shell (*Cyrtospirifer brodi*, MRAN 6162-12, *ventral valve*); G: detail of the fibres in cross section, fibre with a neat profile has been marked in yellow (*Cyrtospirifer brodi*, MRAN 6162-12, dorsal valve); H: detail of the fibres, fibre with a neat profile has been marked in yellow (*Cyrtospirifer* cf. C. *kermanensis*, MRAN 6162-18, ventral valve); I: enlarged detail of the fibres (*Hedeinopsis* sp. ind., MRAN 6904-5, ventral valve). Ext: external part of the shell; Int: internal part of the shell.

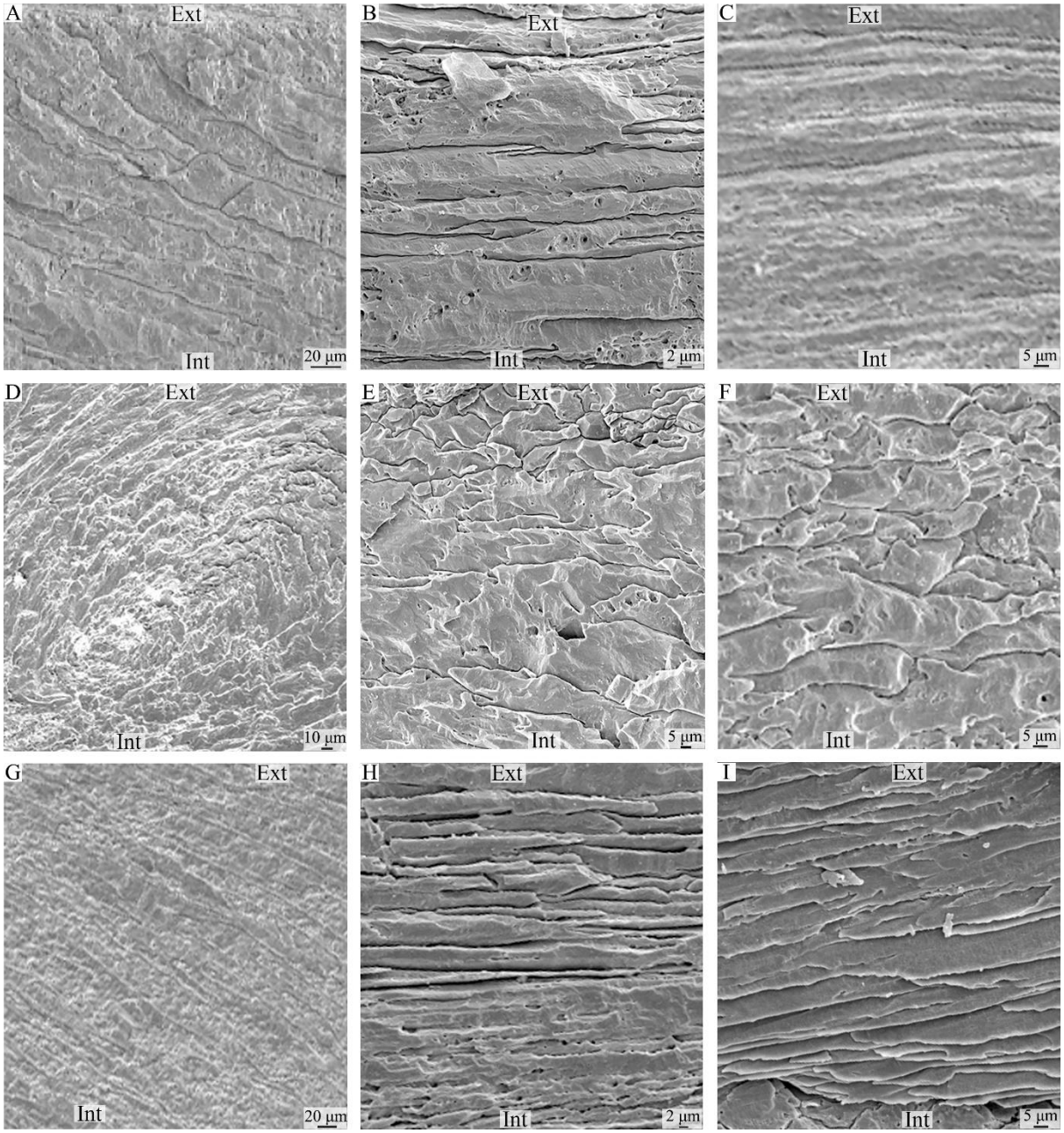

Fig. 10. A, B: fibrous layer in the posterior and central part of the shell respectively (*Hesperonomiella* sp. ind., MRAN 8761-3, ventral valve); C: longitudinal section of the fibrous layer in the anterior part of the shell (*Isorthis* sp. ind., MRAN 6903-1, ventral valve); D: fibrous layer in the posterior part of the shell (*Clorinda molongensis*, NiB5-10A, ventral valve); E, F: fibrous layer in the central and anterior part of the shell respectively (*Syntrophioides* sp. ind., MRAN 8291-5, ventral valve); G: fibrous layer in the posterior part of the shell (*Cyphoterorhynchus arpaensis*, MRAN 6162-10, ventral valve) H, I: longitudinal section of the fibrous layer (*Rhynchotrema* sp. ind., MRAN 6784-1, ventral valve). Ext: external part of the shell; Int: internal part of the shell.

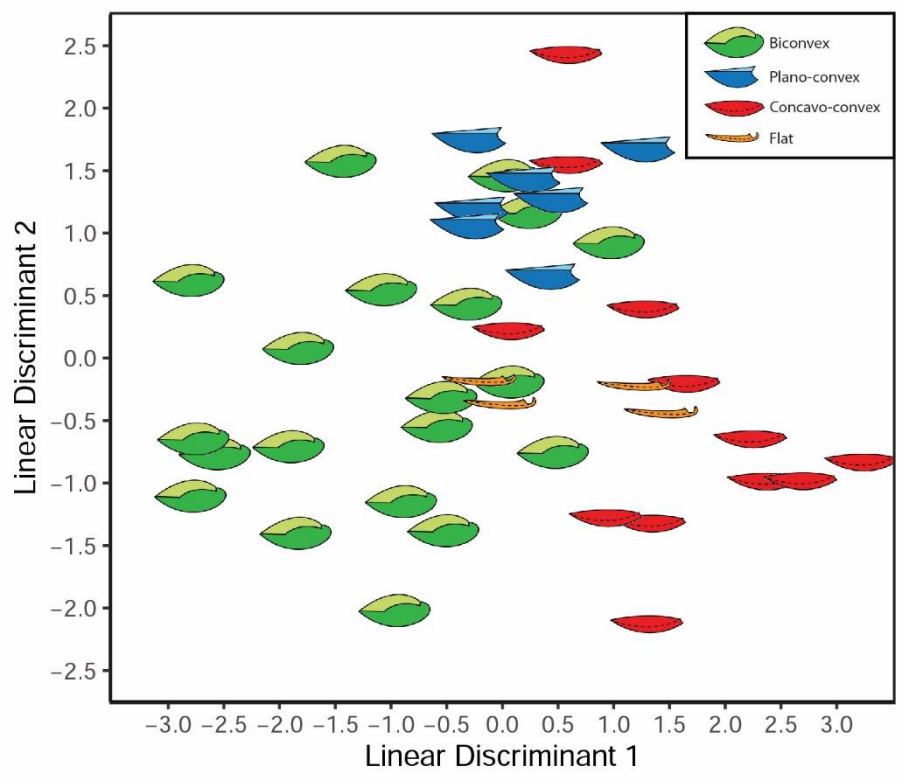

Fig. 11. Plot of the Linear Discriminants 1 and 2 for the specimens included in the dataset employed to build the model.

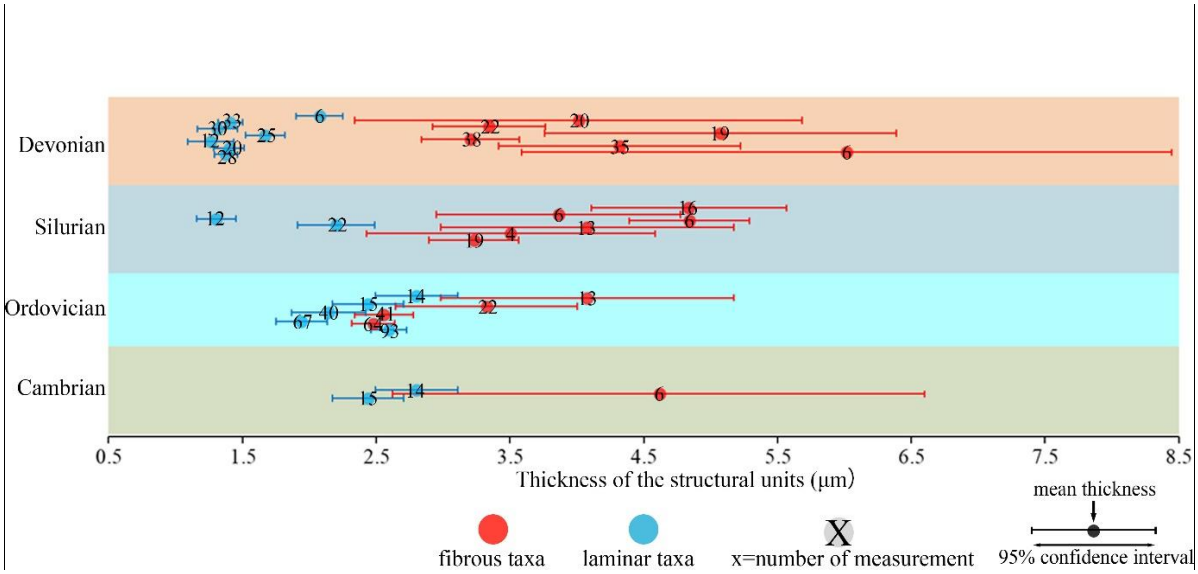

Fig. 12. Thickness of the structural units of the secondary fabrics from the Cambrian to the Devonian; every dot represents the mean value of each species; fibrous and laminar taxa are shown in red and blue colour respectively; the number on each dot represents the number of measurements; the length of bars reflects the size of the confidence interval.

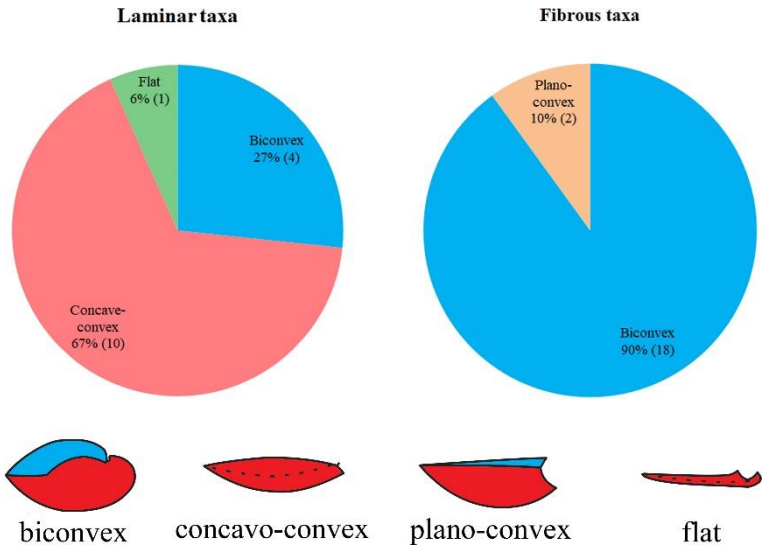

Fig. 13. Pie chart illustrating the numerical proportion of shell shape for the laminar (left) and fibrous (right) fabrics; the percentages refer to the number of species, which are in parentheses. Different brachiopod shell shapes (red: ventral valve; blue: dorsal valve).

Table 1. Taxonomy, geological age, shell shape and main microstructural features of the analysed fossil specimens.

Sample Name	Order	Class	Age	Shape of shell	Layers	Other microstructure	Number of Individual	Sampling localities
Billingsella aff. *B. seletensis* (Nikitin, 1956)	Billingsellida	Strophomenata	Cambrian	Biconvex	laminar		4	Shirgesht (34°12’32”N, 56°48’20”E)
Billingsellidae gen. et sp. ind.	Billingsellida	Strophomenata	Middle Cambrian to the Lower Ordovician	Concave-convex	laminar		2	Haftanan (32°27’47.8”N,49°55’53.7”E)
Protambonites cf. *P. primigenius* (Havlíček, 1972)	Billingsellida	Strophomenata	Late Cambrian to Early Ordovician	Biconvex	laminar	pseudopunctae?	2	Haftanan (32°27’47.8”N, 49°55’53.7”E)
Martellia shabdjerehensis (Percival et al., 2009)	Billingsellida	Strophomenata	Ordovician	Biconvex	laminar, columnar layer?	spines	6	Shabdjereh (31°04’35.1”N,56°09’58”E)
Leptellina sp. ind.	Strophomenida	Strophomenata	Ordovician	Concave-convex	laminar, columnar layer?	pseudopunctae?	4	Shabdjereh (31°04’35.1”N, 56°09’58”E)
Ingria sp. ind.	Strophomenida	Strophomenata	Late Ordovician	Flat	laminar, columnar layer?		2	Shirgesht (34°12’32”N,56°48’20”E)
Leptaena depressa (Sowerby, 1825)	Strophomenida	Strophomenata	Silurian	Concave-convex	laminar		2	Shirgesht (34°12’32”N, 56°48’20”E)
Productella cf. *P. belanskii* (Stainbrook, 1943)	Productida	Strophomenata	Devonian	Concave-convex	laminar, columnar layer?	pseudopunctae? spines?	2	Poldasht (39°03′31.1″N, 45°17′07.3″E)
Productella cf. *Productella subaculeata* (Murchison, 1840)	Productida	Strophomenata	Devonian	Concave-convex	Laminar, columnar layer?	spines?	1	Nasrolah (34°36′52.9″N, 57°11′17.7″E)
Productella sp. ind.	Productida	Strophomenata	Devonian	Concave-convex	laminar	pseudopunctae? spines?	5	Shotori (33°20’14”N, 57°20’28”E) Anarak (33°11’05”N, 53°53’30”E)
Rhytialosia sp. ind.	Productida	Strophomenata	Devonian	Concave-convex	laminar	pseudopunctae	1	Nasrolah (34°36′52.9″N, 57°11′17.7″E)
Spinulicosta sp. ind.	Productida	Strophomenata	Devonian	Concave-convex	laminar	pseudopunctae?	2	Nasrolah (34°36′52.9″N, 57°11′17.7″E)
Striatochonetes sp. ind.	Productida (Chonetidae)	Strophomenata	Devonian	Concave-convex	laminar	pseudopunctae?	3	Jam (35°44’10”N,53°48’41”E)
Devonochonetes sp. ind.	Productida (Chonetidae)	Strophomenata	Devonian	Concave-convex	laminar, columnar layer?		3	Soh (33°29’45”N,51°33’44.5”E)
Triplesia alata (Ulrich and Cooper, 1936)	Orthotetida (Triplesiidina)	Strophomenata	Silurian	Biconvex	laminar		1	Shirgesht (34°12’32”N,56°48’20”E)
Hesperonomiella sp. ind.	Orthida	Rhynchonellata	Middle Cambrian to Early Ordovician	Biconvex	fibrous		3	Haftanan (32°27’47.8”N,49°55’53.7”E)
Nicolella actoniae (Sowerby, 1839)	Orthida	Rhynchonellata	Ordovician	Plano-convex, Concave-convex	fibrous, columnar layer?	punctae?	4	Shirgesht (34°12’32”N,56°48’20”E)
Paralenorthis sp. ind.	Orthida	Rhynchonellata	Ordovician	Plano-convex	fibrous, columnar layer?		9	Shabdjereh (31°04’35.1”N,56°09’58”E)
Howellites ultima (Bancroft, 1945)	Orthida	Rhynchonellata	Late Ordovician	Biconvex	fibrous, columnar layer?	punctae?	2	Shirgesht (34°12’32”N, 56°48’20”E)
Isorthis (Ovalella) inflata (Hairapetian et al., 2012)	Orthida	Rhynchonellata	Early Silurian	Biconvex	fibrous, columnar layer?		2	Shirgesht (34°12’32”N, 56°48’20”E)
Isorthis sp. ind.	Orthida	Rhynchonellata	Early Silurian to Early Devonian	Biconvex	fibrous		2	Zarand (30°51’48”N,56°39’00”E)
Syntrophioides sp. ind.	Pentamerida	Rhynchonellata	Late Cambrian	Biconvex	fibrous		2	Galikuh (32°58’45.8”N,49°36’48.8”E)
?*Clorinda* sp. ind.	Pentamerida	Rhynchonellata	Silurian	Biconvex	fibrous		2	Shirgesht (34°12’32”N,56°48’20”E)
Clorinda molongensis (Mitchell, 1921)	Pentamerida	Rhynchonellata	Silurian	Biconvex	fibrous		3	Shirgesht (34°12’32”N,56°48’20”E)

Spinatrypina sp. ind.	Atrypida	Rhynchonellata	Silurian to Late Devonian	Biconvex	fibrous	5	Shirgesht (34°12’32”N, 56°48’20”E)
Spinatrypina cf. *S. chitralensis* (Reed, 1922)	Atrypida	Rhynchonellata	Devonian	Biconvex	fibrous	2	Nasrolah (34°36′52.9″N, 57°11′17.7″E)
Rhynchotrema sp. ind.	Rhynchonellida	Rhynchonellata	Late Ordovician and Middle Silurian	Biconvex	fibrous	1	Zarand (30°51’48”N,56°39’00”E)
Stegocornu denisae (Hairapetian et al., 2012)	Rhynchonellida	Rhynchonellata	Silurian	Biconvex	fibrous	2	Zarand (30°51’48”N, 56°39’00”E)
Cyphoterorhynchus arpaensis (Abramian, 1957)	Rhynchonellida	Rhynchonellata	Devonian	Biconvex	fibrous	1	Nasrolah (34°36′52.9”N, 57°11′17.7”E)
Hedeinopsis hispanica hispanica (Gourvennec, 1990)	Spiriferida	Rhynchonellata	Silurian	Biconvex	fibrous	3	Shirgesht (34°12’32”N, 56°48’20”E)
Hedeinopsis sp. ind.	Spiriferida	Rhynchonellata	Silurian	Biconvex	fibrous	1	Zarand (30°51’48”N,56°39’00”E)
Cyrtospirifer brodi (Venjukov, 1886)	Spiriferida	Rhynchonellata	Devonian	Biconvex	fibrous	1	Nasrolah (34°36′52.9”N, 57°11′17.7”E)
Cyrtospirifer cf. *C. kermanensis* (Brice, 1999)	Spiriferida	Rhynchonellata	Devonian	Biconvex	fibrous	5	Nasrolah (34°36′52.9”N, 57°11′17.7”E) Behabad (31°54’35”N,55°53’53.6”E)
Cyrtospirifer sp. ind.	Spiriferida	Rhynchonellata	Devonian	Biconvex	fibrous, columnar layer?	2	Behabad (31°54’35”N,55°53’53.6”E)
Uchtospirifer aff. *Uchtospirifer nalivkini* (Lyashenko, 1957)	Spiriferida	Rhynchonellata	Devonian	Biconvex	fibrous, columnar layer?	1	Behabad (31°54’35”N, 55°53’53.6”E)

Table 2. Results of Dunnett's Modified Tukey-Kramer Pairwise Multiple Comparison between the thickness of structural units among specimens belonging to different taxonomic groups. The alpha significant level is settled to 0.05.

	Mean difference	95% CI	Sign of difference
Strophomenata vs Rhynchonellata	1.8	1.3 – 2.2	negative
Billingsellida vs Other Laminar taxa	0.5	0.1–1.0	positive
Orthida vs Other Fibrous taxa	1.4	0.8–2.0	negative

Table 3. Relationships between shell shapes and secondary layer fabrics.

Laminar		Fibrous	
Biconvex	4	Biconvex	18
Concavo-convex	10	Concavo-convex	0
Flat	1	Plano-convex	2

Table 4. Linear discriminant coefficients for the variables included in the model, plotted in Fig. 12.

	LD1	LD2	LD3
Log of shell thickness	-0.39	1.05	-0.17
Structural unit thickness	-0.95	-0.24	0.61
Size	-0.47	-0.37	0.22
Aspect Ratio	-0.49	-0.23	-0.95

Table 5. Correlation coefficients between the shell thickness and the thickness of the structural units at order (and specific) level.

	Shell thickness		**Log of shell thickness**	
Order	**r**	***p*-values**	**r**	***p*-values**
BILLINGSELLIDA	-0.72	0.17	-0.69	0.19
PENTAMERIDA	-0.43	0.72	-0.33	0.78
STROPHOMENIDA	0.24	0.61	0.30	0.51
PRODUCTIDA	0.46	0.15	0.34	0.31
ORTHIDA	**-0.60**	**0.05**	**-0.70**	**0.02**
SPIRIFERIDA	-0.08	0.82	0.03	0.93
Species				
Cyrtospirifer cf. *C. kermanensis*	0.74	0.26	0.74	0.26
Martellia shabdjerehensis	-0.14	0.91	-0.21	0.87
Striatochonetes sp.	-0.67	0.53	-0.67	0.53